Final Draft
of the original manuscript:

Comprehensive screening of Mg corrosion inhibitors

S.V. Lamaka[1]*, B. Vaghefinazari[1], Di Mei[1], R.P. Petrauskas[1], D. Höche[1], M.L. Zheludkevich[1,2]

[1]*Magnesium Innovation Centre - MagIC, Helmholtz-Zentrum Geesthacht (HZG), 21502 Geesthacht, Germany*
[2]*Institute for Materials Science, Faculty of Engineering, Kiel University, Kiel, Germany*

Abstract

This work presents the results of a systematic screening for magnesium corrosion inhibitors. The ability to form stable soluble complexes with $Fe^{ii/iii}$ was considered on first place when choosing the compounds for hydrogen evolution tests. Inhibiting effect of 151 individual compounds was tested towards six alloys (AZ31, AZ91, AM50, WE43, ZE41 and Elektron 21) and three grades of pure magnesium. Newly identified and previously reported inhibitors are ranked by their inhibiting efficiency and compared with Cr (VI) reference. A number of new inhibitors are discovered with efficiency exceeding that of chromate.

*Corresponding author: +49 4152 871914, **Sviatlana.Lamaka@hzg.de**

Keywords: Magnesium corrosion • corrosion inhibition • magnesium inhibitor •magnesium complex• chelate

1. Introduction

Efficient surface and coating technology for magnesium is a well-known challenge. Surface pre-conditioning [1], [2-5] and various types of coating technologies [6-8] are typically adapted to fit the requirements given by the magnesium material application and possible corrosion exposure scenarios. These facts indicate that a more general viable technology would be a great benefit. Such a technology can be achieved by efficient corrosion inhibitors embedded into various types of conventional surface treatments [8-10]. However, efficient and environmentally friendly corrosion inhibitors are lacking. Reviews on corrosion inhibitors for Mg alloys are scarce: perhaps, only one comprehensive review has been published recently [11]. The challenge is that often literature provides dissimilar data describing the effect of the same inhibitor on different Mg alloys or even controversial data for the same Mg alloy. Meanwhile, the field of Mg corrosion inhibitors develops rapidly. Novel inhibition systems for magnesium are reported regularly [12-22]. In particular adsorption and barrier effects of anionic surfactants [13, 14, 23] have shown high corrosion inhibition efficiency due to blocking the species exchange between the electrolyte and anodic/cathodic surface areas. Theoretically, a purely anodic acting inhibitor would be of great interest and is expected to be very efficient. Such an inhibition system would need a very fast interaction kinetic in order to suppress the anodic dissolution of Mg (typically α-phase). As shown by theoretical studies from Chen et al. [24] the strong and fast adsorption of hydroxyl ions on electrochemically active Mg surfaces is a determining step for the Mg interaction kinetics. This fits well to statements of Taylor and Francis [25, 26] derived via atomistic studies on chemisorption properties of involved ions on top of hexagonal closed packed Mg surfaces in frame of water dissociation reaction schemes. Even highly reactive fluoride ions, typically used in conversion coating treatments [27, 28], compete with OH^- ions [29] during passive film formation. No inhibiting system is known

up to now which fully satisfies the requirements of efficient passivation of the anodic α-phase in Mg corrosion since the affinity to react with species like O_2, OH^- or H_2 is high [30].

However there is another possibility to suppress the corrosion process: inhibition of cathodic activity. This approach was also found to be efficient for different aluminium alloys [31-36]. Given that noble inclusions (e.g. Fe, Cu, Ni) present in magnesium based engineering materials, act as cathodes, the suppression of their activity can be the key for efficient corrosion inhibition. Recently, we have shown that initial cathodic process on Fe-rich particles and anodic dissolution of Mg around it leads to the loss of galvanic protection and detachment of iron particles from magnesium substrate by undermining. Self-corrosion of detached Fe-rich particles occurs with formation of $Fe^{II/III}$. These species can be reduced to metallic Fe and re-plated back to Mg substrate creating Fe patches. This leads to growth of the total cathodic area and acceleration of general corrosion process [37]. Binding $Fe^{II/III}$ by specific complexing agents prevents Fe re-plating and greatly inhibits magnesium corrosion. The efficiency of this general approach to corrosion inhibition has been already validated [17].

In this paper we continue investigating the role of iron complexing agents on corrosion inhibition of Mg. These were considered on the first place at the inhibitor pre-selection stage since Fe is known as the most relevant impurity also because it is the most difficult to get rid of in the processing chain. Although we briefly discuss the inhibiting mechanism of some suggested inhibitors, it is out of the scope of this paper to study the mechanistic details of all the tested compounds. Rather, the aim of this work is to set up an extensive inhibitor database (with ranking by inhibition efficiency on various Mg-based substrates) for future detailed studies and outline the applications not only for the inhibitors but also for the substances accelerating dissolution of Mg.

2. Experimental Part

Given that corrosion and hence inhibition mechanism can vary significantly depending on the composition of Mg based material, a number of industrially important magnesium alloys and pure magnesium with different amount/distribution of impurities were tested. The magnesium alloys ZE41, AZ31 and Elektron 21 (hereafter E21) from ingot casting (for wrought applications), and cast magnesium alloys WE43, AZ91 and AM50 were used as substrates for testing the inhibiting efficiency. Additionally, two types of high purity Mg (HP-Mg-50ppm and HP-Mg-51ppm) and commercial purity magnesium CP-Mg-220 were tested. A SPECTROLAB spark discharge optical emission spectroscopy device (SD-OES) with "Spark Analyser Vision" software was used to determine the average elemental compositions. All the measurements were repeated 3 times on 3 different samples of the same material resulting in 9 values for each element. The samples for analysis were taken from different sections of the ingots. The analytical chemical composition of all the metallic substrates was determined by optical emission spectroscopy and presented in **Table 1**.

The ingots of HP-Mg-51ppm, HP-Mg-50ppm, WE43, ZE41, E21, AZ31, AZ91 and AM50 were milled to produce small metallic chips with the effective surface area of 240 to 550 cm^2/g. This was done to ensure high surface area and the identical chemical composition of each portion of the alloy used for testing inhibiting efficiency. Due to different mechanical properties of the alloys and varying settings of the shaving equipment, the surface area of the chips received from each of the alloys varied. The representative testing chips are shown in **Fig.1**.

Commercial purity magnesium (CP-Mg-220ppm) was tested as plates. Bare material was cut into coupons of 5.0 cm^2/g, abraded with 1200 grade silicon carbide paper, rinsed with ethanol and dried in a stream of compressed air. The effective surface area of each tested material is presented in **Table 2**.

Table 1. Chemical composition of pure Mg and alloys as analysed by spark (optical) emission spectroscopy. The values are in ppm or in at. % when indicated.

Element	CP-Mg-220ppm	HP-Mg-51ppm	HP-Mg-50ppm	WE43	ZE41	E21	AZ31	AZ91	AM50
Ag	<1	0,71±0,27	0,5	32±2	9±2	31±3	<1	<1	<1
Al	130±15	50±6,2	34,1±2,5	133±4,7	144±10,1	145±7,3	2,86±0,05%	7,95±0,29%	4,83±0,03%
Ca	4±3	<1	3±2,9	225±5,0	27±0,3	42±0,7	5	10±2,2	6
Ce	<4	<4	<7	206±4,7	0,65±0,03%	70±19,1	9	<9	<9
Cu	5±3	<1	<1	47±4,2	19±0,5	20±0,7	14±0,5	48±8,6	13±0,6
Fe	220±30	51±1,1	50±2,2	38±7,2	15±8,3	12±2,3	17±3,5	22±6,7	9±0,83
La	<5	<5	<5	0,14±0,01%	0,42±0,02%	26±9,1	<2	<2	3±1,9
Mn	150±65	8±3,8	8±1,2	60±2,2	79±2,2	38±1,2	0,36±0,01	0,23±0,01	0,40±0,02%
Ni	<2	<2	<2	46±1,9	7±4,7	52±5,2	3±0,9	<2	3,4±1,9
Pb	<4	<4	11±2,4	92±3,1	7±4,0	18±8,1	-	-	8
Si	53±45	<1	2±1,3	0,92±0,2	2±2	4±4,5	271±28,5	561±87,1	590±10
Sn	3±2	<3	4±0,7	38±1,9	49±2,8	70±3,5	<5	24±7,8	<5
Zn	4±2	10±15,5	36±0,9	268±11,6	4,2±0,1%	0,29±0,01%	0,74±0,01%	0,54±0,04%	349±13,6
Zr	5±4	23±12,2	<5	0,17%±0,02	0,30±0,01%	0,19±0.01%	<6	<6	18±2,2
Mg	99,94%	99,98%	99,98%	92,85±0,13%	93,75±0,17%	96,09±0,01%	96,00±0,06%	91,20±0,32%	94,67±0,03%
Pr		-	-	0,10±0,002%	647±36	340±11			
Th		-	-	0,15±0,002%	0,29±0,003%	920±35			
Ti		-	-	78±0,7	12±1,3	34±1,9			
Y		-	-	4,49±0,12%	50±0	72±5,6			
Nd				1,95±0,03%	0,24±0,01%	3.2±0,2%			

Fig. 1. Visual appearance of 0.5 g of testing materials with the surface area of 400 cm^2/g.

Hydrogen evolution tests were performed using eudiometers (art. nr. 2591-10-500 from Neubert-Glas, Germany). 0.50 g of chips or a coupon of CP-Mg-220 was put in the electrolyte container (500 ml) of eudiometer. The electrolyte was constantly stirred at 350 ± 100 rpm. The immersion electrolyte contained 0.5 wt.% sodium chloride with or without inhibitor. In most cases 0.05M solution of inhibitor in NaCl was used. In

some special cases less concentrated or saturated solutions ($C_{inh} < 0.05M$) of inhibitors were prepared. Hydrogen evolution tests were repeated 6 times in pure NaCl solution and normally performed once for the electrolytes containing potential corrosion inhibitor. The best inhibitors were then re-tested two or three times to confirm the results.

Table 2. Average surface area of each tested Mg material.

Material	CP-Mg-220ppm	HP-Mg-51ppm	HP-Mg-50ppm	WE43	ZE41	E21	AZ31	AZ91	AM50
Surface area, cm²/g	5.0	550	240	400	490	360	180	430	550

The main goal of this study was to examine the inhibiting efficiency towards Mg corrosion of a wide range of chemical compounds. Following our previous work [17] the selection of potential inhibitors was based mainly on their ability to form soluble complexes or precipitates with Fe^{2+} or Fe^{3+}. Apart from that, chemical compounds previously reported to have inhibiting effect on Mg corrosion (Referenced within **Table 3**) were tested for reference and general ranking. All chemical compounds tested were purchased from commercial suppliers (mostly from Sigma-Aldrich) and used without additional purification. Amount of reagent necessary to prepare 0.05M solution was added to 0.5% NaCl solution and stirred until it dissolves. The pH of all the electrolytes was adjusted by NaOH or HCl to the values varying between 5.5 to 7.2, controlled by Metrohm-691 pH meter equipped with Mettler-Toledo LabExpert Pt-1000-pH glass electrode. Hence, all the chemicals purchased as acids were tested as their sodium salts.

The metallographic samples of HP-Mg-51ppm, HP-Mg-50ppm and CP-Mg-220ppm were prepared by grinding the coupons with SiC paper to 4000 grit finish and then consecutive polishing in 3 μm diamond suspension (Schmitz) and in a mixture of 1μm diamond and OPS™ suspension (Fumed Silica Suspension 0.2 μm water free). Scanning electron microscope (TESCAN Vega3 SB) combined with an energy dispersive spectrometer (EDS) from eumeX (iXRF Systems) was used to examine the microstructure of Mg materials.

3. Results and discussion

3.1 Inhibitor screening results

Hydrogen evolution as a function of immersion time in 0.5% NaCl solution was used as an inhibitor performance measure. Although time-consuming, it does not require application of external polarization and does not imply the use of carcinogenic chromic acid necessary for cleaning corroded magnesium for weight loss measurements. Besides, hydrogen evolution measurements usually correlate well with the weight loss measurement for Mg materials because one mole of dissolved magnesium generates one mole of hydrogen gas [38]. Most of the compounds were tested at concentration of 0.05M. Some were also tested at lower concentrations if 0.05M solutions could not be prepared due to the limited solubility or lower concentration was earlier reported to have higher inhibiting efficiency. The duration of the tests was 22 to 78 hours, the cut off time for calculating all the inhibiting efficiencies was established at 20h. The example of hydrogen evolution curves in pure 0.5 wt.% NaCl is given in **Fig. 2**.

Average (of six measurements) volume of H_2 evolved after 20h was determined and used for subsequent calculations of the inhibiting efficiency. Based on the results of hydrogen evolution tests, the inhibiting efficiency (η) of each inhibitor was defined by the following equation:

$$\eta = \frac{V_{H_2}^0 - V_{H_2}^{Inh}}{V_{H_2}^0} \cdot 100\%$$

where $V_{H_2}^0$ and $V_{H_2}^{Inh}$ are the amounts of H_2 (ml) evolved at 20 hours of immersion in pure NaCl solution and in NaCl solution containing corrosion inhibitor. The values of calculated inhibiting efficiency are given in **Table 3**.
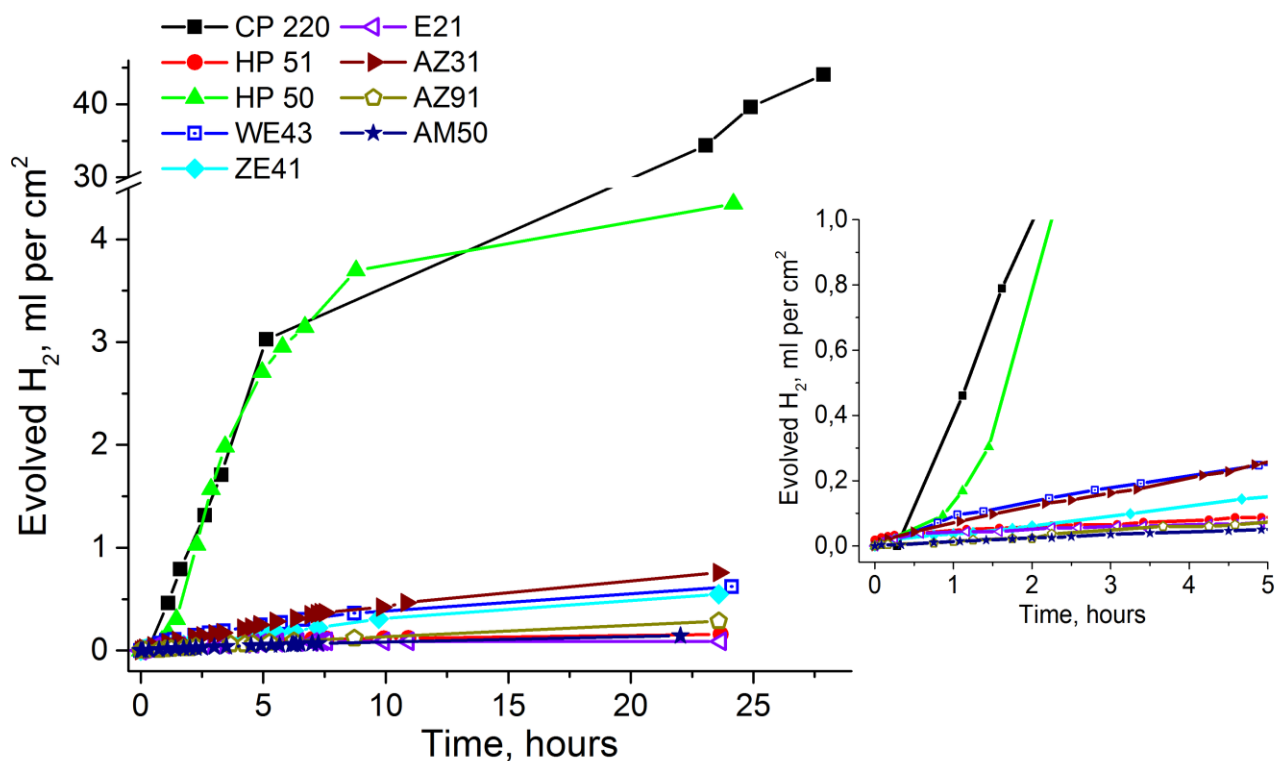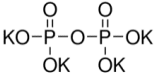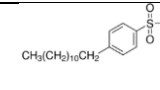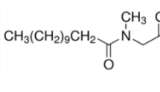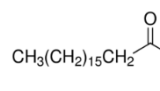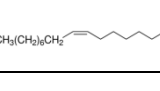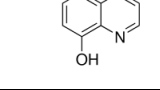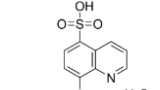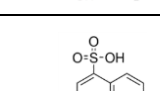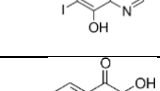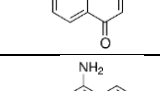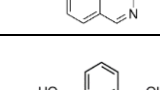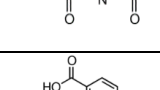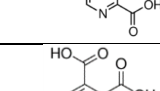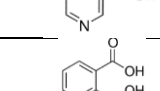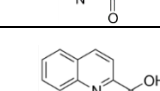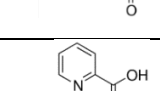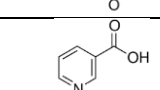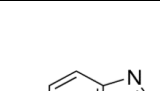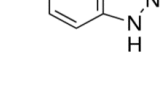

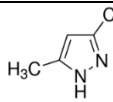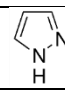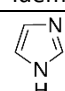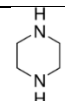**Fig. 2.** Normalized hydrogen evolution rate in 0.5% NaCl for nine tested Mg materials.
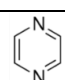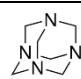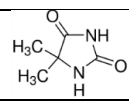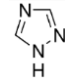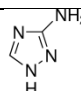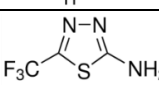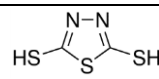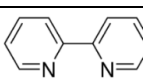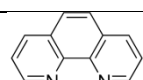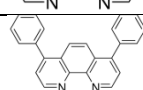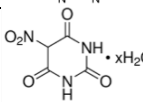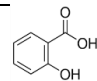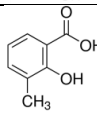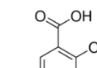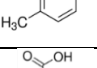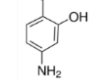
Positive inhibitor efficiency indicates that corrosion was retarded while negative values mean that corrosion was accelerated. The table also contains the structural formulas of corresponding compounds, and references in case the substance had been previously reported as magnesium corrosion inhibitor.
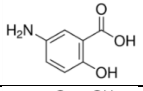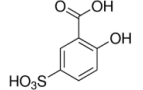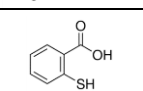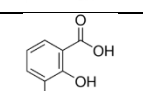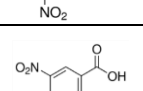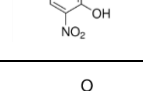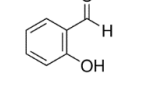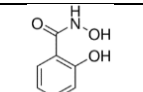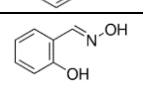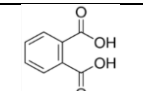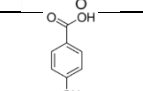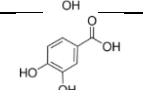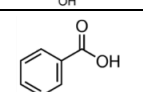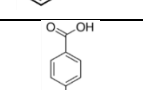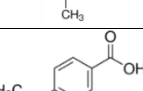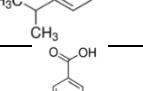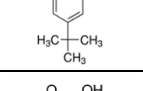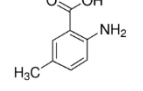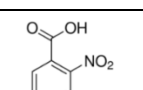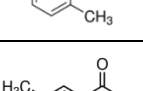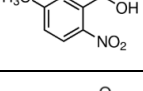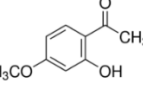
Although a number of compounds demonstrated high inhibiting efficiency, they should not be immediately recommended for industrial application. Verification of environmental amiability of each new inhibitor is critical when making the decision about its wide applicability. The information about the acute toxicity and carcinogenicity provided in **Table 3** was extracted from safety data sheets (SDS) for corresponding reagents (mostly from sigmaaldrich.com). Chemical substances are divided in five categories of toxicological severity based on LD50 (50% lethal dose) measured in mg/kg of bodyweight [39]. The gradations are the following: Category 1 – 5 mg/kg; 2 – 50, 3 – 300, 4 – 2000, 5 – 5000 mg/kg. Note, that even if the chemical compound is neither toxic nor carcinogenic nor mutagenic, it still might be harmful to environment (e.g. like $Ce(NO_3)_3$ or Salicylaldehyde). The statement "not identified" in **Table 3** is a short form of carcinogenicity statement in SDS that literally reads as "No component of this product present at levels greater than or equal to 0.1% is identified as probable, possible or confirmed human carcinogen by IARC". Toxicity to fish usually considers LC50 (50% lethal concentration). When not available, EC50 level is shown (half maximal effective concentration) for fish or for daphnia or other aquatic invertebrates. As explained above, all the acids were neutralized for the measurements to pH 5.5 to 7.2. But the toxicological information for the reagents bought (usually acid) is shown in **Table 3**. Note that toxicity of salts is usually lower than that of acids.
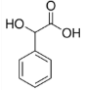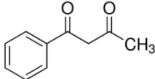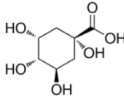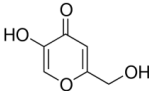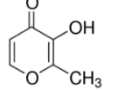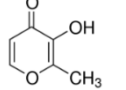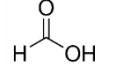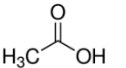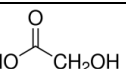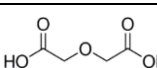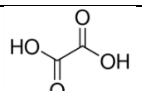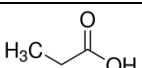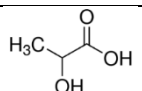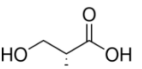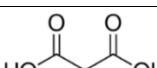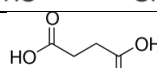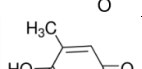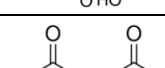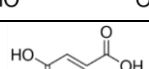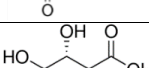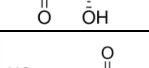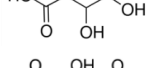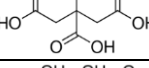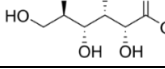
Table 3. Inhibiting efficiency (η, %) of all tested compounds for nine Mg substrates. Positive inhibiting efficiency indicates that corrosion was suppressed, while negative values correspond to accelerated dissolution of Mg. The inhibiting efficiency was calculated based on the H₂ evolution values after 20h in 0.5% NaCl at 23.3 ± 1.9 ºC. All the compounds described as "acid" and amino-acids were tested at initial pH 5.5 to 7.2 ad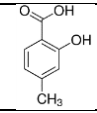justed by NaOH, making tested compounds sodium salts of specified acids. The pH values after the immersion test (Final pH) are also shown but only for CP-Mg-220ppm.
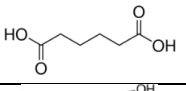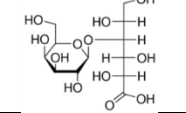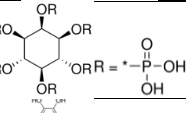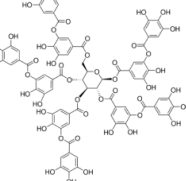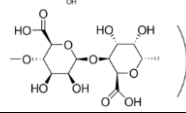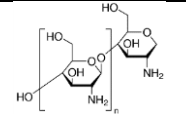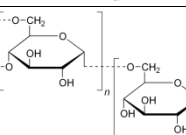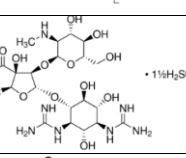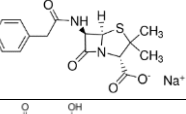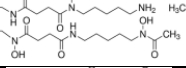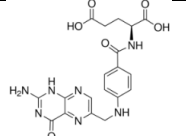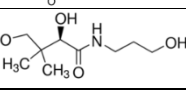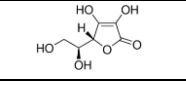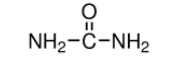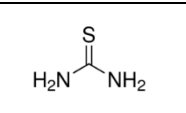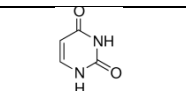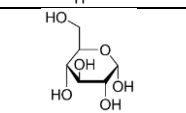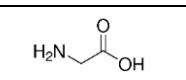
Chemical Compound, Concentration / Repetitions	CP-Mg-220ppm Final pH	CP-Mg-220ppm IE, %	HP-Mg-51ppm	HP-Mg 50ppm	WE43	ZE41	E21	AZ31	AZ91	AM50	Structural formula	Acute Toxicity LD50 Oral ^{rat}, mg/kg / Carcinogenicity / Toxicity to fish, mg/l	Reference
Na₂CrO₄ 0,05M (Cr (VI) – reference)	6,6	61	85	56	80	-39 ±19	62	94	88	82		52 / Carcinogenic to humans / 17,6	[8, 40]
KNO₃ 0,05M **2**	11,0	97 ±1	8	97	88 ±2	95 ±3	75	86 ±7	69 ±24	87 ±10		3750 / Probably carcinogenic to humans / 22,5 Harmful to aquatic life	[41],[42],[43]
KNO3 0,005M	11,6	17			25	-9	36	85	71	65			
KNO₂ 0,05M	10,9	77			70	53	89	95	82	79		157,9 / Probably carcinogenic to humans / 0,94 Very toxic to aquatic life	[42]
KCN (initial pH 7.5) 0,05M	10,5	94										7,49 / Not identified / 0,11 Very toxic to aquatic life with long lasting effects	[17]
K₃Fe(CN)₆ 0,05M	10,9	60	-474	70	-48	-4	-419	60	8	13		2970 ^{mouse} / not identified / 869	
NaSCN 0,05M	10,6	59 ±10			14	7	-317	6	-21	-112		764 / Not identified / 233	[17]
NaF 0,05M	11,7	67	16	93	55	75	11	71	42	45		148,5 / Toxic if swallowed / Not identified 200	[40, 44-46]
Na₃PO₄ 0,05M	7,6	71±7			-31	-45	-878	-176	-251	-359		n/a Not identified n/a	[40, 47]
Na₃PO₄ 0,01M **2**	8,7	93±1	-71	90	27±3	43 ±22	-181 ±6	19 ±11	-10 ±2	-59 ±8			
Na₃PO₄ 0,0002M	11,4	86			33	51	20	77	65	60			
K₄P₂O₇ (Pyrophosphate) 0,05M	12,3*			41	-142	-40		-334		-714	KO–P(=O)(OK)–O–P(=O)(OK)–OK	2980 $^{[48]}$ / Not identified / > 100	
K₄P₂O₇ (Pyrophosphate) 0,02 M	8,7	49	-292	69	-49	-69	-770	-182	-243	-443			
Na₂SO4 0,05M	11,3	68			46	68	-77	56	60	30		5989 / Not identified / 120	[47]
NaHCO3 0,002M	10,7*			54	0	34	-146	44	38	22			[47]
Na₂MoO₄ 0,05M	11,9*		14		-181	4	-1704	-65	-103	-197			[49, 50]
NaVO₃ 0,05M	9,8*			90	-6	4	-360	-58	-9	-167			[51, 52]
CeCl₃ 0,05M	7,1	-8	-993	-13	-321	-223	-2789	-755	-703	-1174		n/a Not identified n/a	[8, 15]
CeCl₃ 0,01M	9,7*		-707	6	-174	-225	-2040	-487	-370	-676			
CeCl₃ 0,005M **2**	10,2	-16 ±22	-546	-1	-73	-781	-1514	-432	-275	-1524			
Ce(NO₃)₃ 0,05M **3**	6,1	92 ±3	-26	90	70 ±7	62 ±1	62 ±7	83 ±12	73 ±9	2 ±21		4200 / Not identified / 0.3 Very toxic to aquatic life with long lasting effects	[45]
Ce(NO₃)₃ 0,005M **3**	7,4	58 ±7	-19 ±9	85 ±2	33 ±2	-4 ±7	-709 ±33	23 ±6	-58 ±9	44 ±8			
La(NO₃)₃ 0,05M	7,9	88			49	45		38	60	-39		410 $^{Intraperitoneal Mouse}$	
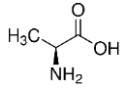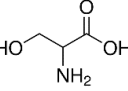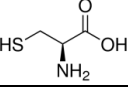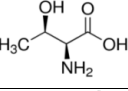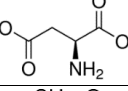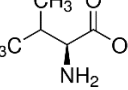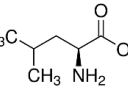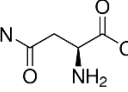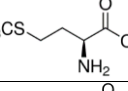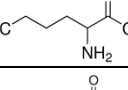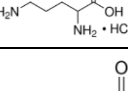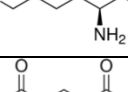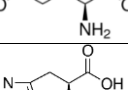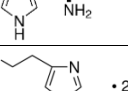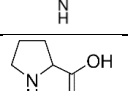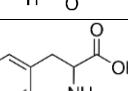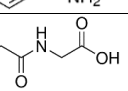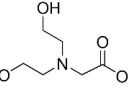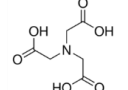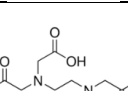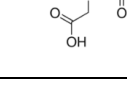
Name	pH										Structure	Toxicity	Ref
La(NO₃)₃ 0,005M **2**	10.0	-1	-17 ±10	81 ±1	13 ±10	-32 ±16	-625 ±38	12 ±10	-22 ±5	18 ±0		Not identified n/a	
LaCl₃ 0,05M	7,9	-43			-305	-252	-2751	-645	-663	-1167		4184	
LaCl₃ 0,005M **2**	9,6	-12	-444	-1±6	-92±4	-196 ±18	-1298 ±74	-348 ±65	-241 ±18	-551 ±63		Not identified n/a	
Dodecylbenzene Sulfonic acid 0,05M	11,2	93	6	70	49	53	40	63	67	57	CH₃(CH₂)₁₀CH₂—⬡—SO₂—ONa	500 Not identified 3,2	[13, 14, 53],[46, 54]
N-Lauroylsarcosine Na 0,04M	10,8	17	47	88	47	70	64	60	4	38	CH₃(CH₂)₉ CH₃ ONa	5000 Fatal if inhaled Not identified 107	[13]
Stearic acid 0,02M	10,3	61	-26	79	-13	-150	-50	-201	-118	-236	CH₃(CH₂)₁₅CH₂—COOH	2000 Tumorigenic in tests on mouse n/a	[23]
Oleic acid 0,01M	8,3	70			64	27	65	39	38	-4	CH₃(CH₂)₆... OH	74000 Not identified 205	[16]
8-Hydroxyquinoline Saturated (0,01M)	9,7	95	-93	90	-10	-75			-6	-71		1200 Potentially mutagenic 18	[14, 46, 53, 55-59]
8-Hydroxyquinoline 0,005M	10,9	16			4	-58	-127	-16	-13	-60			
8-Hydroxy-5-quinoline-sulfonic acid 0,025 M	11,0	1	-179	50	-71	-119	-668	-208	-183	-330		n/a Not identified n/a	
8-Hydroxy-7-iodo-5-quinolinesulfonic acid 0,025 M	7,6	53	-107	76	-25	-32	-487	-64	-102	-181		4000 Not identified n/a	
8-Hydroxy-7-iodo-5-quinolinesulfonic acid 0,05M	11,9	84											
2-Hydroxy-1,4-Naphtoquinone 0,04 M	10,4	17	48	97	34	-30	-42	90	60	33		2520 Not identified 420	
5-Aminoisoquinoline 0,002 M	10,7		15		20	-41	9	47	-2	16		n/a Not identified n/a	
2,6-Pyridinedicarboxylic (Dipicolinic) acid 0,05M	11,1	90										n/a Not identified n/a	[60]
2,6-Pyridinedicarboxylic (Dipicolinic) acid 0,03M	11,0	82	75	99	73	71	69	79	65	69		322	
2, 5- Pyridine-dicarboxylic (Isocinchomeronic) acid 0,05M **2**	10,9	83 ±11	92 ±2	99 ±1	83 ±1	52 ±3	83 ±3	84 ±1	68 ±3	70 ±4		n/a Not identified n/a	[60]
3,4-Pyridinedicarboxylic (Cinchomeronic) Acid 0,038M	11,0	80	64	97	71	57	81	82	67	74		n/a Not identified n/a	[60]
2,3-Pyridinedicarboxylic (Quinolinic) acid 0, 05M **3**	11,1	64 ±3	70 ±4	98 ±1	51 ±3	32 ±5	54 ±18	62 ±1	47 ±9	47 ±3		n/a Not identified n/a	[60]
Quinaldic acid 0,05M **2**	11,2	85	70	51	62 ±17	21 ±38	70 ±5	86 ±11	74 ±12	77 ±9		n/a equivocal evidence for germ cell mutagenicity	[55]
Quinaldic acid 0,015M		55										n/a	
Picolinic acid 0,05M	11,4	21			41	54	47	54	45	22		750 Not identified n/a	
Nicotinic acid 0,05M (Niacin or Vitamin B3)	10,8	66	13	80	18	3	-19	37	24	27		6450 Not identified 520	
Benzotriazole 0,05M	9,6	29	-504	43	-218	-108	-1372	-340	-257	-646		560 Equivocal tumorigenic agent 25 Harmful to aquatic life with long lasting effects	[16, 61-64]
Benzotriazole 0,02M	9,3	23	-251	58	-125	-74	-851	-131	-222	-289			
Benzotriazole 0,005M	10,2	-2			-19	-63	-220	-70	-39	-142			
Benzotriazole 0,0005M	10,9	14			-15	-19	-7	24	40	21			
5-chlorobenzotriazole 0,01M	10,9	38±6			-5	-12	-255	9	-8	-65		n/a Not identified	[16]
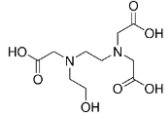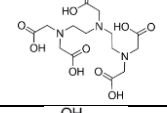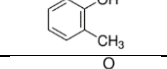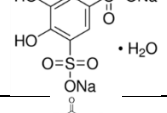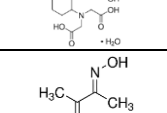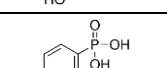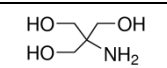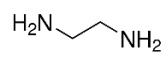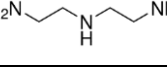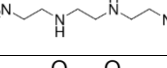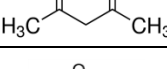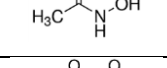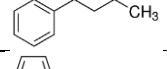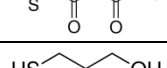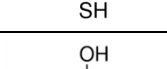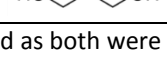
Compound	pH										Structure	Toxicity	Ref
5-chlorobenzotriazole 0,001M	10,2*			0	20	-68	-55	-77	26	-13		n/a	
3,5- Dimethylpyrazole 0,05M	10,8	0	-20	9	8	-67	6	-43	-27	-42		1060 Not identified n/a	[64, 65]
Pyrazole 0,05M	11,0	27 ±13			4	-38	25	20	31	8		1010 Fetotoxicity 111	[64]
Pyrazole 0,005M	10,8*			0	30	-74	18	-76	38	11	idem	idem	idem
Imidazole 0,02M	10,2	-78			-100	-125	-754	-352	-302	-603		970 Presumed human reproductive toxicant 280	
Piperazine 500 ppm	10,3	-11	-110	-1	-43	-88	-252	-93	-26	-103		2600 Not identified 1800	[12]
Piperazine 0,05M	10,1	-34	-352	-24	-119	-145	-1045	-318	-106	-414	idem	idem	idem
Pyrazine 500 ppm	10,8	-45	19	1	-16	-6	69	57	51	61		2730 intraperitoneal Not identified n/a	[12]
Hexamethylenetetramine (Urotropine) 0,11 M 16g/l	11,1	-67			-18	-35	-29	14	24	4		20000 Not identified 49000	[66]
5,5-Dimethylhydantoin 0,05M	9,5	-28	-796	8	-221	-172	-2152	-467	-355	-678		5000 Not identified 972,2	
1,2,4-Triazole 0,05M	10,0	24	-733	32	-206	-183	-1254	-275	-43	-177		1648 Not identified 760	[3, 16, 45, 64, 65, 67]
3-Amino-1,2,4-triazole	9,9	23 ±19			-87	-157	-975	-222	19	-144		25000 Possibly carcinogenic >100	[16]
2-animo-5-trifluoro-methyl-1,3,4-thiadiazole Saturated	10,7	8										n/a Not identified n/a	
1,3,4-thiadiazole-2,5-dithiol (DMTD, Bismuthiol I) 0,05M	10,0	55		67	-79	-17		-74		-218		intraperitoneal 200 mouse Not identified n/a	
2,2' Bipyridyl 0,05M 2	10,7	31 ±40			42	6	31	43	47	35		100 Not identified n/a	
1,10-Phenanthroline 0,005M	10,7	5±3			52	-63	18	21	59	31		132 Not identified n/a	
Bathophenanthroline 0,0005M	11,0	-18			-3	-41	-3	-83	11	-43		n/a Not identified n/a	
5-Nitrobarbituric Acid 0,05M 2	9,3	82	8	79 ±7	71 ±6	51 ±27	-175 ±60	77 ±9	71	74 ±16		n/a Not identified n/a	
Salicylic Acid 0,05M 2	11,3	92	-22 ±20	86±2	14±3	37±7	-259 ±47	36±1	26±2	-97 ±21		891 Not identified > 500	[17, 68]
3-Methylsalicylic 0,05M	10,9	97	28	94	52	75	-25 ±20	78	52	66		445 Not identified n/a	[69]
4-Methylsalicylic 0,05M	11,0*		-17	89	36	39	-205 ±31	36	9	41		1800 Not identified n/a	[69]
5-Methylsalicylic acid 0,05M	10,4	72	61	90	76	55	76	59	56	29		1000 Not identified n/a	[17, 69]
5-Methylsalicylic acid 0,032M	11,1*		20	93	64	59		60	52	47			
4-Aminosalicylic acid 0,05M 2	10,5	85±1	16 ±11	87±4	50 ±12	57±9		56±8	52±1			4000 Not identified n/a	[69]

8

Compound	pH	1	2	3	4	5	6	7	8	9	LD50 / Toxicity	Ref
5-Aminosalicylic acid 0,05M	11,0	86	33	85	33	66	14	83	80	77	2800 Not identified n/a	[69]
5-Sulfosalicylic Acid 0,05M	11,4	60	-460	46	-131	-50		-73	-125	-737	n/a Not identified n/a	[69, 70]
Thiosalicylic acid 0,005M	9,8	86		89	-33	-64	-78	42	49	29	n/a Not identified	
Thiosalicylic acid 0,002M	10,8	-3	-124	83	12	-27	25	66	67	54		
3-Nitrosalicylic acid	11,4	28			65	51	17	68	74	68	n/a Not identified n/a	[69]
3,5 - Dinitrosalicylic acid 0,05M	9,5	12 ±1			66	38	-158	3	15	-27	860 Not identified n/a	[69]
3,5-Dinitrosalicylic acid 0,002M 2	11,2	54 ±26	81	36	63 ±1	11 ±32	82 ±6	64 ±3	86 ±1	81 ±2		
Salicylaldehide 0,05M	9,1	98	31		95		82	25	18	-67	520 Not identified 2,3 Toxic to aquatic life with long lasting effects	
Salicylalhydroxamic acid 0,05M	8,1	75	-213	64	-69	-17	-562	-197	-177	-701	5000 Limited evidence of carcinogenicity in animal studies	
Salicylaldoxime 0,05M	9,1	55	-75	41	41	-89	-226	-351	-265	-421	n/a Not identified 3.23	[55]
Phthalic acid 0,05M	11,2	41	-36	90	-20	31	-181	36	33	10	n/a Not identified n/a	
4-Hydroxybenzoic acid	10,1	10			-281	-170	-1868	-399	-261	-623	10000 Not identified > 99,4	
3,4-Dihydroxybenzoic acid 0,05M	9,1	-12	-989	-3	-344	-270	-2949	-696	-800	-1119	n/a Not identified n/a	[70]
Benzoic Acid 0,05M	10,8*		48	84	24	34	51	58	40	70	2360 Not identified 44.6 Harmful to aquatic life	[53, 54, 64]
p-Toluic acid 0,05M	10,4	49	-204	86	25	-6	-194	-21	-39	20	2340 mouse Not identified n/a	[64]
4-Isopropylbenzoic acid (Cuminic acid) 0,005M	9,5	73 ±25	51	94	25	-79	17	84	62	24	n/a Not identified n/a	[64]
4-tert-butylbenzoic acid 0,05M	12,0	57±5	-47	25	-18	31	-114	45	-91	9	473 Not identified 4	[64]
2-amino-5-methyl-benzoic acid 0,05M	9,7	-76									n/a Not identified n/a	
2-amino-5-methyl-benzoic acid 0,006M	10,8	-15	32	33	30	-4	4	43	19	28		
3-methyl-2-nitrobenzoic acid 0,05M	10,1	65	-102	50	50	29	-230	43	25	9	n/a Not identified n/a	
3-methyl-2-nitrobenzoic acid 0,03M	10,8	13	-57	39	-30	-10	-776	36	-85	-78		
5-methyl-2-nitrobenzoic acid 0,02M 2	10,1	65±0	12	26	19	11	-173 ±63	90	18	-29	n/a Not identified n/a	
5-methyl-2-nitrobenzoic 0,005M	11,2	-1			2	0	-256	49	3	11		
2'-Hydroxy-4'-methoxyaceto-phenone (Paeonol) 0,05M	10,7	33									490 Not identified 54,9	[19]
2'-Hydroxy-4'-methoxy-acetophenone 50ppm	10,9	41			4	-49	-12	12	12	-2		

Compound	pH										Structure	Toxicity	Ref
Mandelic acid 0,05M	11,2	61	-12	44	-19	-6	-99	38	11	4		4100 intraperitoneal / Not identified / n/a	
1-Phenyl-1,3-butanedione (BenzoylAcetone) 0,05M	10,6	-69										n/a / Not identified / 1,1mg/l	
Quinic acid 0,05M **2**	10,8	59±4	-2	43±29	15	19±48	-25	51±7	37	42±16		Subcutaneous 10000 / Not identified / n/a	
Kojic acid 0,05M	11,1	46	-4	37	18	45	-287	-36	-90	-92		250 / Equivocal tumorigenic / n/a	
Kojic acid 0,02M	9,8	30	-25	48	-39	-3	-364	-124	-118	-249			
Maltol 0,05M	11,0	35	-96	52	-20	9	-589	-183	-168	-408		1410 / Not identified / n/a	
Formic acid 0,05M	10,8*		30	55	34	-5	0	78	19	35		11200 / Not identified / > 954	
Acetic acid 0,05M	11,0	57			10	-17	-1	74	60	50		3310 / Not identified / > 1000	
Glycolic acid 0,05M **3**	11,0	65±13	38±1	63±2	50±3	59±4	-3±8	61±7	49±8	50±13		2040 / Not identified / 5000	
Diglycolic acid 0,05M	10,9	86	6	93	50	60	-31	74	54	59		500 / Not identified / 105	
Oxalic acid 0,05M **2**	11,2	86±4	-29±24	92±1	33±3	52±4	-189±16	65±4	63±8	40±12		1080 / Not identified / 160	[17, 40]
Propionic acid 0,05M	10,6	35±2			19	-29	6	40	34	50		3455,1 / Not identified / n/a	
Lactic acid 0,05M	10,4	48		84	-159	36		-25		-19		n/a / Not identified / n/a	
Glyceric acid, Ca salt 0,05M	11,1	41	43	14	28	24	16	49	57	51		n/a / Not identified / n/a	
Malonic acid 0,05M	10,4	-26		70	-126							1310 / Not identified / 150	
Succinic acid 0,04M	11,0	80±3	9	93	39	43	-33	51	28	30		2260 / Not identified / >100	
Citraconic acid 0,01M	11,0	39±19	13	36	23	-73	-4	-60	2	-16		1320 / Not identified / n/a	
Maleic acid 0,05M **3**	10,9	52±8		86	8±24	12±14	-5±2	12±37	26±1	-21±6		708 / Not identified / 75	
Fumaric acid 0,05M **3**	11,0	84±3	73±12	95±2	87±2	17±3	90±3	90±3	83±2	80±7		9300 / Not identified / > 100	
Tartaric acid 0,05M **3**	10,3	64±23	-90	87±3	-10±3	46±12	-344±94	49±3	52±4	37±19		>2000 / Not identified / 93,31	
Malic acid 0,05M	11,2	74		88	24	34		10		16		5500 / Not identified / n/a	
Malic acid 0,03M	11,1	84	30	87	55	63	-21	65	46	47			
Citric acid 0,05M **2**	10,9	65±7	-319±58	58±3	-80±49	-47±49	-986±313	-66±14	-78±12	-365±32		375 / Not identified / 10	
D-gluconic acid	11,7	58		58		48		19		-97		n/a / Not identified / n/a	

Compound	pH	1	2	3	4	5	6	7	8	9	Structure	Toxicity	Ref
Adipic acid 0,05M	10,8	59	-22	89	21	16	-106	38	-48	12		5560 Not identified 46	
Lactobionic acid	11,2	7		58	59	55	-70	26	48	53		> 5000 Not identified > 100	[59]
Phytic acid 0,05M	7,4	60		66		-42		-191		-226		n/a Not identified n/a	[71]
Phytic acid 5g/L	7,7	64			9	4	-294	-42	-35	-132			
Tannic acid 0,005M	5,91	83	-543	60	-133	-213	-609	-108	-132	-312		2260 Equivocal tumorigenic agent 37	
Alginic acid	11,2	-2										>5000 Not identified n/a	[18, 21]
Chitosan 7,5g/L	6,8	-11	-80	27	-23	-97	-72	30	-2	-2		> 10000 Not identified 1,73 Toxic to aquatic life	
Dextran 0,05M	10,8	-24										n/a Equivocal tumorigenic agent n/a	
Streptomycin sulfate 0,05M	8,3	70	-298	75	-69	-111	-707	-60	-72			430 Suspected human reproductive toxicant >180	
Penicilin G, Na salt 0,05M	9,9*		-357	28	-162	-155	-999	-35	-40	-144		6916 Not identified n/a	
Deferoxamine mesylate 0,02M	10,4	13										17300 Not identified n/a	
Folic acid (Vitamin B$_9$) 0,05M	8,8	85	89	79	52	23	77	58		-10		n/a Not identified n/a	
D-Panthenol (Provitamin B) 0,05M	10,3	-8	-587	4	10	-98	9	-50	-27	-66		15000 Not identified n/a	
Ascorbic acid (Vitamin C) 0,05M	10,6*		-135	87	-56	6	-401	34	38	-85		11900 Not identified n/a	
Urea 0,05M	10,8	-6	24	11	23	-93	18	-69	-19	-40		8471 Not identified 17500	
Thiourea 0,05M	11,1*			60	43	-16	-52	50	57	33		1750 Probably carcinogenic Suspected human reproductive toxicant 10000	
Uracil 0,05M	8,9	-26	-264	52	-111	-108	-900	-294	-151	-671		6000 Not identified n/a	
Glucose 0,05M	10,7	26			14	-43	-52	-7	29	-14		25800 Not identified n/a	
Glucose 0,005M	10,7	30			13	-38	14	20	27	9			
Glycine 0,05M 2	9,6	-43	-955	18±7	-268 ±24	-215 ±12	-965	-353 ±3	-82	-434 ±17		7930 Not identified n/a	[72]

Compound	pH										Structure	Toxicity	Ref
L-Alanine 0,05M	9,9	-21									(structure)	> 5110 Not identified 100	[72]
DL-Serine 0,05M	10,2	14									(structure)	n/a Not identified n/a	
L-Cysteine 0,05M	9,9	29	-389	41	-258	-104	-1287	-155	-206	-575	(structure)	5850 Not identified 100	[72]
L-Threonine 0,05M	10,1	42									(structure)	Intraperitoneal 3098 Not identified n/a	[72]
L-Threonine 0,034 M	9,9	23	-910	37	-257	-276	-1826	-460	-427	-765			
Aspartic acid 0,05M	10,3	14	-371	65	-134	-54	-812	-132	28	-203	(structure)	5000 Not identified n/a	
L-Valine 0,05M	9,7	-23									(structure)	2000 tumor-promoting activity for bladder carcinomas 10000	[72]
L-Leucine 0,05M	9,9	-17									(structure)	> 16000 tumor-promoting activity for bladder carcinomas n/a	[72]
L-Asparagine 0,05M	9,8	1		42		-188		-397			(structure)	n/a Not identified n/a	
L-Methionine 0,05M	9,9	28									(structure)	36000 Not identified n/a	
DL-Norleucine 0,05M	10,3	-43			-113	-138	-710	-327	-127	-322	(structure)	n/a Not identified n/a	
L-Ornithine hydrochloride 0,05M	10,8	-60									(structure)	10000 Not identified n/a	
L-Lysine 0,05M	9,9	60									(structure)	n/a Not identified n/a	
L-Lysine 0,0064 M	10,3	-70	-139	-5	-47	-113	-328	-305	-194	-533			
L-Glutamic acid 0,05M	10,1	7	-119	45	-228	-139	-1054	-229	-84	-198	(structure)	> 5110 Not identified > 100	[72]
L-Histidine 0,05M	10,0	26									(structure)	> 15000 Not identified n/a	
Histamine dihydrochloride 0,007 M	9,6	-65	-114	-1	-61	-154	-296	-240	-156	-592	(structure)	2534 Not identified n/a	
DL-Proline 0,05M	10,2	-34									(structure)	n/a Not identified n/a	
DL-Phenylalanine 0,05M	10,3	16±7	-157	-7	-142	-146	-322	-267	-149	-352	(structure)	n/a Not identified n/a	[72]
Glycylglycine hydrochloride 0,05M	10,0	-48	-282	55	-197	-133	-770	-291	-300	-423	(structure)	7930 Not identified n/a	
Bicine 0,05M	9,5	-52	-295	43	-82	-111	-743	-311	-227	-372	(structure)	Intraperitoneal 1.540 Not identified n/a	
Nitrilotriacetic acid (NTA) 0,05M [2]	10,4	-20	-757	14±9	-296 ±3	-124 ±46	-2755	-315 ±106	-476	-529 ±155	(structure)	1460 Possibly carcinogenic to humans 3100	[70, 73]
K₂EDTA 0,05M	12,0	29	-237	19	-348	-128	-1482	-379	-599	-750	(structure)	4500 Not identified 41	[63, 74],[73], [70]
K₂EDTA 0,02M	10,6	20	-474	55	-112	-82	-1723	-497	-545	-619			
K₂EDTA 0,001M [3]	10,9	18 ±2			14 ±9	-24 ±8	-29 ±13	-18 ±17	-21 ±44	-25 ±12			

Inhibitor	pH*										Toxicity	Ref.
N-(2-hydroxyethyl)ethylenediamine-N,N',N'-triacetic acid (HEDTA) 0,05M	12,0	6									Intraperitoneal 337 / Not identified / 852	[70]
Diethylenetriaminepenta acetic acid (DTPA) 0,05M	11,0	-75									> 2.000 / Suspected human reproductive toxicant / >100	[70]
3-Methylcatechol 0,05M	9,8	-1	4	16	-7	-31	-1261	-105	-129	-167	n/a / Not identified / n/a	
Tiron (Pyrocatechol-3,5-disulfonate Na) 0,05M	9,0	-80			-295	-244	-2736	-609	-644	-1046	1320 / Not identified / n/a	[73],[70]
Tiron 0,0072M	10,3	63										
1,2-Diaminocyclo-hexanetetraacetic acid (DCTA) 0,05M	10,4	-2			-296	-238	-2544	-614	-710	-1075	Intraperitoneal 413 / Not identified / n/a	[70]
Dimethylglyoxime 0,05M	10,3	22									250 / Not identified / n/a	
PhenylPhosphonic acid 0,05M	10,4	18									2000 / Not identified / n/a	[40]
TRIS(Tris(hydroxymethyl)-aminomethane)	10,2	-72			-255	-194	-1981	-569	-596	-1013	3000 / Not identified / >100	
Ethylendiamine 0,05M	9,7	-61									1200 / Not identified / 115,7	
Diethylentriamine (DETA) 0,05M	9,7	17		73	-36	-18		-139		-1788	1080 / Not identified / 1014	[75]
Triethylenetetramine 0,05M	9,6	-67									2500 / Not identified / n/a	
Acetylacetone 0,05M	10,7	-23									570 / Not identified / 106	
Acetohydroxamic acid (AHA) 0,05M	10,8	6									Intraperitoneal > 2000 / Presumed human reproductive toxicant / n/a	
1-Phenyl-1,3-butanedione 0,05M	10,7	-69									n/a / Not identified / 1,1	
2-Thenoyltrifluoroacetone 0,005M	10,3	37	63	13	52	-52	32	21	71	42	n/a / Not identified / n/a	
2,3-Dimercapto-1-propanole 0,05M	9,9	48									217 mouse / Not identified / n/a	
Glycerol 0,05M	11,1	19	11	2	21	-13	33	9	24	13	12600 / Not identified / n/a	

* When CP-Mg-220ppm was not tested, the final pH values for HP-Mg-50ppm are reported as both were similar.

For the inhibitors tested twice or three times, the error magnitude decreases when the inhibiting efficiency increases. The reproducibility of the results is in the range of 5% to 20% for the cases when inhibiting efficiency was above 40%. However, the error increases when the inhibiting efficiency was low or negative. This trend of increased error at lower inhibiting efficiency was also observed by Muster et al [76] for Al corrosion inhibitors.

3.2 Why corrosion rate and inhibiting efficiencies differs markedly for two grades of high purity Mg?

Although the amount of Fe, Cu and Ni impurities is very similar in two types of high purity magnesium, HP-Mg-50ppm and HP-Mg-51ppm, **Table 1**, they show completely different corrosion and inhibition behaviour, **Fig. 2**, **Table 3**. Judging by the corrosion rate, HP-Mg-50ppm is similar to commercial purity magnesium CP-Mg-220ppm containing 220 ppm Fe. The amount of Mn and Si in HP-Mg-50ppm and HP-Mg-51ppm is also similar, but the content of Al and Zr in HP-Mg-51ppm is significantly higher, 50 and 23 ppm respectively, while in HP-Mg-50ppm these elements account only to 34 and <5 ppm correspondingly. On the other hand, HP-Mg-50ppm contains higher amount of Zn and Pb. In any case, these differences in bulk content of impurities can barely explain significant difference in corrosion and inhibition behaviour of two high purity magnesium substrates. Elemental composition of impurity particles found in three types of pure Mg suggests better explanation, **Table 4**.

Table 4. Elemental composition of impurity particles in pure Mg as shown by EDS, at.%.

Substrate / Element	Atomic %								
	CP-Mg-220ppm			HP-Mg-51ppm			HP-Mg-50ppm		
	Low* Fe	High Fe	Average of 14	Low Fe	High Fe	Average of 7	Low Fe	High Fe	Average of 9
Mg	87,2	42,9	**72,0 ±18,5**	95,48	77,4	**86,1 ± 8,1**	83,5	76,1	**82,4 ± 6,6**
Al	0,54	4,56	**2,1 ± 1,7**	0,37	10,47	**5,2 ± 4,9**	0,17	0,23	**0,18 ± 0,07**
Si	3,8	13,3	**6,7 ± 4,2**	0,21	11,39	**6,1 ± 5,1**	5,8	6,5	**4,8 ± 1,9**
Mn	0,19	0,61	**0,33 ± 0,17**	0,025	0,031	**0,02 ± 0,01**	0,09	0,132	**0,10 ± 0,05**
Fe	7,4	38,4	**18,2 ±12,9**	0,14	0,45	**0,34 ± 0,15**	9,1	16,2	**11,4 ± 4,9**
Ni	0,19	0,16	**0,23 ± 0,06**	0,12	0,06	**0,10 ± 0,05**	0,32	0,32	**0,29 ± 0,09**
Cu	0,20	0,20	**0,10 ± 0,07**	0,030	0,002	**0,03 ± 0,02**	0,29	0,18	**0,27 ± 0,10**
Zr	0,41	0,01	**0,24 ± 0,61**	3,09	0,05	**1,91 ± 1,88**	0,09	0,31	**0,35 ± 0,40**
Pb	0,02	0,01	**0,05 ± 0,07**	0,53	0,12	**0,27 ± 0,16**	0,59	0,01	**0,24 ± 0,40**

* low and high values of at. % correspond not to the lowest and the highest values detected, but to more representative average low and average high values of at.% .

The size of the impurity particles in all three pure magnesium material vary between 0,5 to 3 micron with the average size of 1 micron. Besides, the agglomerates of Fe impurity particles reaching ca. 100 micron were also found in CP-Mg-220ppm. Fe-rich impurity particles were found and analysed by SEM/EDS. Note that Mg is not expected to make part of the impurity particle, but due to the small size of the impurity particles, EDS also gives the info about the matrix. Impurity particles in CP-Mg-220ppm are abundant and typically are very rich in Fe (3 to 43 at.%) accompanied by Si (2 to 14 at.%) and either Al or Zr (average 2,1 and 0,24 at.% correspondingly). These Fe-rich impurity inclusions are the initial points of micro galvanic corrosion. They act as local cathodes favouring radial dissolution of Mg around each particle. Local concentration of Mg^{2+} and OH^{-} is the highest in these sites resulting in precipitation of $Mg(OH)_2$ on Fe-rich impurities, **Fig.3**. Similarly, the impurities in HP-Mg-50ppm are also rich in Fe (3 to 19 at.%) accompanied by Si (1 to 8 at.%) and Zr (average

0,35 at.%) but low in Al (average 0,18 at.%). On the contrary, the impurity particles in HP-Mg-51ppm are rare, with low Fe content (average 0,34 at.%) accompanied by high Si, Al and Zr content (average 6,1, 5,2 and 1,9 at.% correspondingly).

The presence of different micro-alloying elements in the Mg-based substrates can significantly affect the composition of Fe-containing precipitates and consequently their electrochemical activity as local cathodes. Aluminium even at low concentrations influences the impact of Fe by forming Al-Fe compounds that are less cathodically active. These can be e.g. Al_3Fe or $Al_xMn(Fe)$/ $Al_x(Mn-Fe)$ phases depending on the alloy. The ratio of Fe/Mn in these compounds is also important for stoichiometric reasons and efficient secondary phase formation [77]. The oxidation properties of such phases weaken the effect of iron on local galvanic corrosion. The impact of Si on Mg corrosion does not relate to the formation of Mg_2Si phases. Silicon only has an impact on the availability of Fe-rich particles since it promotes their formation in solidifying magnesium [78]. This is also the reason for the enrichment of Si in such particles. The addition of Zr for grain refinement is well described [79]. Besides, Zr can purify Mg melt by forming Fe_2Zr or $FeZr_2$ compounds and thus decreasing corrosion activity of Fe [80]. However, in high amounts detrimental micro-galvanic coupling can occur and Zr can become a corrosion hotspot [81]. More detailed information on the influence of secondary inclusion on Mg corrosion can be found elsewhere [82-84].

Summarising, low content of Fe accompanied by relatively high content of Al or Zr, made Fe-containing impurities in HP-Mg-51ppm only mildly active in initiating micro-galvanic corrosion. On the contrary, Fe-rich impurities in HP-Mg-50ppm and CP-Mg-220ppm effectively initiated micro-galvanic corrosion. These matches the general trend of the data presented in **Table 3**: correlation between inhibiting efficiency values for HP-Mg-51ppm and HP-Mg-50ppm is lower (R^2 = 0,22) than that for CP-Mg-220ppm and HP-Mg-50ppm (R^2 = 0,50).
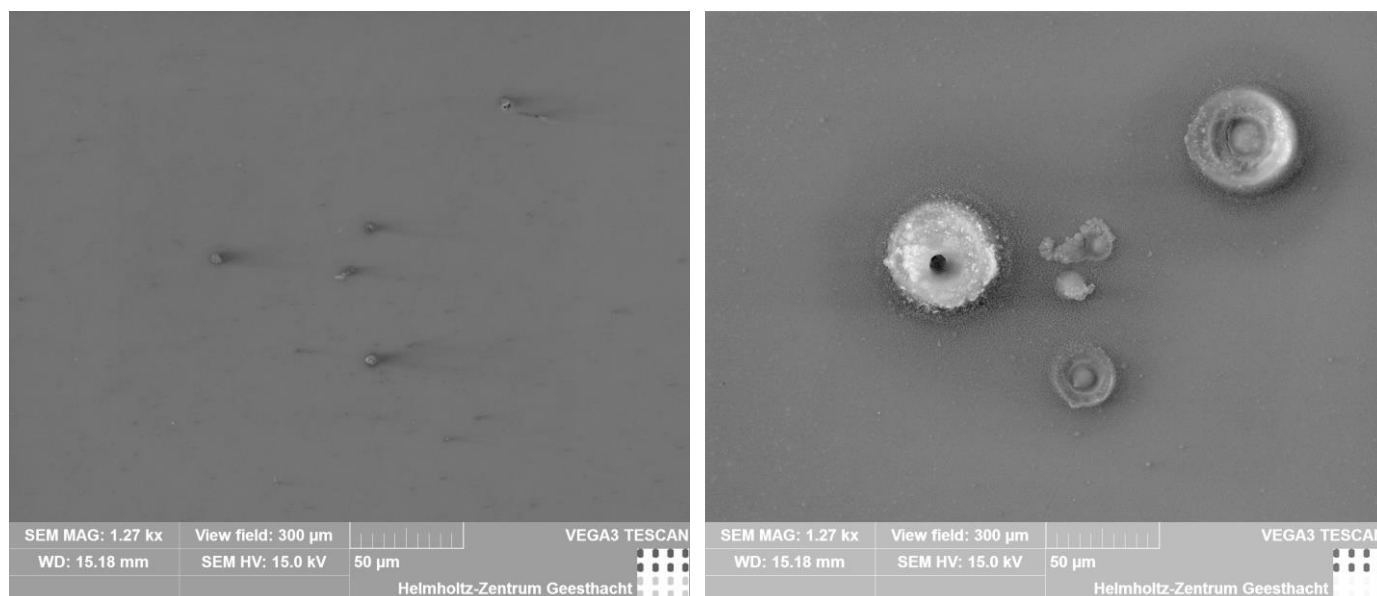
Fig. 3. Iron-rich impurities in CP-Mg 220 before and after 30 minutes of immersion in 0.5% NaCl. The same site is shown. The initial Fe content in five impurity particles varied between 3,2 to 37,3 at.%.

3.3. Discussion on inhibitors performance

Carcinogenic chromate Na_2CrO_4 (initial pH = 6.2), tested here as a reference demonstrated efficiency in the range of 60% to 90% with the exception of ZE41 alloy to which CrO_4^{2-} repeatedly showed negative inhibiting efficiency accelerating corrosion process.

Nitrate and nitrite (both described in SDS as "probably carcinogenic to humans") showed high inhibiting efficiency of 70% to 95%. Although both, NO_3^- and NO_2^- were previously reported [41, 43, 85] as effective Mg corrosion inhibitors, the inhibiting mechanism is not clear yet. In [43] it was argued that

inhibiting mechanism of NO_3^- cannot be related to the competitive adsorption between NO_3^- and Cl^-. Given that both, NO_3^- and NO_2^- are commonly used inhibitors for steel effective at high pH, and in light of significant influence of Fe on corrosion of Mg, we presume that inhibiting effect of NO_3^- and NO_2^- on Mg might be related with interference in Fe oxidation/reduction/replating cycle in the course of Mg corrosion. This is indirectly corroborated by the fact that NO_3^- showed the lowest inhibiting efficiency in case of HP-Mg-51ppm with the lowest content/activity of Fe in the impurity particles. Lower concentration of KNO_3 (0,005M instead of 0,05M) results in much lower inhibiting effect for commercial purity CP-Mg-220ppm and all RE alloys, while remaining at roughly the same level for aluminium containing alloys.

CeCl$_3$ and LaCl$_3$ greatly accelerated corrosion of all nine Mg substrates. Comparing 0,05M and 0,005M solutions of lanthanide chlorides, detrimental effect reduces along with decreasing CeCl$_3$ and LaCl$_3$ concentration. In contrast, 0,05M La(NO$_3$)$_3$ and especially Ce(NO$_3$)$_3$ do show reasonable inhibiting effect to most of the Mg substrates, again excluding HP-Mg-51ppm. In majority of cases, inhibiting efficiency significantly decreases once concentration of La(NO$_3$)$_3$ and Ce(NO$_3$)$_3$ decreases to 0,005M. Comparing the inhibiting efficiency of lanthanide nitrates and chlorides, and inhibiting efficiency of KNO$_3$, it is likely that inhibiting effect of La(NO$_3$)$_3$ and Ce(NO$_3$)$_3$ is mostly caused by NO_3^- rather than RE cation, though a synergistic effect of Ce^{3+} or La^{3+} with NO_3^- cannot be excluded. Detrimental influence of CeCl$_3$ on corrosion of AZ31 has been also recently reported by Williams et al [15], while Supplit et al [3] reported negative influence of Ce(IV) acetate incorporated in silane coating applied on AZ31. Inhibiting mechanisms of lanthanide salts (including Ce and La chlorides [34, 86, 87] and nitrates [36, 55]) described for Al alloys implies formation of Ce(OH)$_3$ or La(OH)$_3$ precipitates on cathodic (Cu-rich) particles and on Al matrix due to elevated local pH [36, 86-88]. Given that high alkalinization accompanies Mg corrosion, it was assumed that lanthanides possess inhibiting effect also for Mg substrates. Multiple experimental reports confirmed that once deposited in optimized conditions, ceria based conversion coatings provide effective barrier for bare or PEO treated Mg alloys [7, 8, 56, 89-92]. Deposition is often done from acidic solutions (pH 3.6 to 4) due to the hydrolysis of cerium salts at higher pH. However, under immersion conditions used in this work, when dissolution of Mg and alkalinization of bulk electrolyte occurred very rapidly due to the high surface area of Mg, Ce^{3+} or La^{3+} did not allow for sufficient increase of pH on Mg surface which is needed to stabilise Mg(OH)$_2$. This is because OH^-, formed as product of water reduction reaction, are consumed to form Ce(OH)$_3$/Ce(OH)$_4$ and La(OH)$_3$ *in diffusion layer or in bulk solution*, rather than on Mg surface. Note that pH of the electrolyte was below 8 for all lanthanide salts after 24 hours of immersion, while stabilization of Mg(OH)$_2$ occurs at pH 10.0 - 10.5.

The anionic surfactants, sodium salts of dodecylbenzenesulphonic acid and N-lauroylsarcosine, showed inhibiting efficiency above 50% for most of the tested alloys. It has been previously shown [13] that these systems possess double inhibiting functionality in contact with Mg: rapid adsorption on Mg surface and formation of sparingly soluble compounds with Mg^{2+}. Resulting protective layer blocks anodic dissolution of Mg and cathodic water reduction. Ability of unsaturated fatty acid - oleic acid - to form thin adsorption layer and inhibit commercial purity Mg was also described in [16]. We observed the same positive effect of oleic acid on CP-Mg 220 ppm and RE alloys, while its inhibiting effect on Al-containing alloys was lower. Surprisingly, saturated analogue of oleic acid - stearic acid - demonstrated similar inhibiting effect for CP-Mg-220ppm and HP-Mg-50ppm, but adverse effect on HP-Mg-51ppm and all RE- and Al-containing alloys, **Table 3**.

8-hydroxyquinoline (8-HQ) and its derivatives chelate a number of di- and tri-valent cations including $Fe^{2+/3+}$ and Mg^{2+}. Interesting, that the trivial name of 8-Hydroxy-7-iodo-5-quinolinesulfonic acid is Ferron as it used for spectrophotometric determination of Fe^{3+} [93, 94]. 8-HQ and its derivatives did not inhibit corrosion of the RE- and Al-containing alloys but showed inhibiting efficiency of 90% for CP-Mg-220pm and HP-Mg-50ppm with the high content of Fe in the impurity particles. The same effect was observed for the sulfo- and sulfo- / iodo- derivatives of 8-HQ tested in this work. Similarly, in [56] it was observed that corrosion

accelerates in presence of 8-HQ loaded in PEO layer formed on ZK30 alloy. In contrast to this, inhibiting effect of 8-HQ was reported for AZ91 [14, 59], AZ31[57], MA8 [58] and ZK30 [46]. The discrepancy with previous works in this case is likely to be explained by combination of adsorption/precipitation inhibiting mechanism of 8-HQ and high rate of corrosion due to the high surface area of samples used in this work. It was shown in [14, 46] that formation of protective layer due to adsorption of 8HQ on AZ91 and ZK30 alloys is a slow process lasting for hours. Precipitation of $Mg(Q)_2$ accompanies adsorption. Precipitation of $Mg(Q2)$ starts at pH >7.6 [95] with the pH range of complete precipitation of Mg^{2+} being 9,4 - 12,7 and solubility product of $Mg(Q2)$ = $6.8 \cdot 10^{-16}$ [55]. In the conditions of fast Mg dissolution observed in our work, slower adsorption process is dominated by formation of sparingly soluble $Mg(Q)_2$ chelates *in the electrolyte* rather than on Mg surface. This accelerates dissolution of Mg. In case of CP-Mg-220pm and HP-Mg-50ppm materials, corrosion was controlled by the rate of the cathodic reaction and high inhibiting effect was achieved because cathodic reaction on Fe-rich impurities was suppressed by dampening the $Fe/Fe^{2+}/Fe^{3+}$ redox cycle. In any case, 8-HQ is not likely to find any industrial applications because it is light sensitive and is equivocally mutagenic according to SDS data.

Benzotriazole (BTA) was tested in a wide concentration range of 0.05M to 0.0005M. At concentration of 0.05M BTA accelerated dissolution of most Mg materials. Corrosion acceleration diminished linearly with decrease of BTA concentration. Weak inhibiting effect for the alloys was only observed at low concentration of 0.0005M. More hydrophobic derivative, 5-chloro-benzotriazole exhibited slightly better performance at the concentration of the same range. Inhibiting effect of benzotriazole (BTA) on Mg corrosion has been first mentioned in [64] and then described in [63]. It was shown that the inhibiting efficiency decreases to zero at 0.05M concentration while at concentration of 0.03M, the inhibiting efficiency reaches maximum of 40%. The results from [63] cannot be directly compared with recent studies on AMLite [62] that show corrosion acceleration of BTA at pH 3 and pH 7 with inhibiting effect evident only at pH 10. Note, that in our testing conditions, pH did not raise above 9.8 after 24 hours for all the tested alloys. Slight corrosion acceleration of CP Mg in borate buffer in presence of BTA was also described in [16]. In any case, BTA is not likely to find any industrial application because it suffer from photon induced degradation when exposed to UV irradiation [96], is marked in SDS as equivocally tumorigenic agent and harmful to aquatic life with long lasting effects.

Nitrobarbituric acid exhibited high inhibiting effect for most of the alloys. It is known analytical reagent for gravimetric determination of Mg as it forms $Mg(NB)_2 \cdot 8H_2O$ [97] which is a sparingly soluble complex. Based on this property, nitrobarbiturate can be grouped together with F-, PO_4^{3-}, $C_2O_4^{2-}$, dodecylbenzenesulphonate, N-lauroylsarcosine and 8-hydroxyquinoline as they all form stable precipitates with Mg^{2+} and might contribute to Mg inhibition via suppressing anodic dissolution. Phosphate (or more precisely the mixture of hydro- and dihydro-phosphates because initial Na_3PO_4 solution was adjusted to pH=7.0) demonstrate weak inhibiting effect at concentration of 0.05 and 0.01M while much better results were achieved at lower concentration of phosphate (0.0002M). This is because at higher concentrations, phosphate buffered the pH at 8.7, which is below the value necessary for stabilization of $Mg(OH)_2$.

Amino-, methyl-, thio-, nitro- and dinitro-derivatives of salicylic acid generally showed high inhibiting efficiency for most of the tested Mg materials. This is likely to be related with suppressing iron re-deposition activity. Salicylic and sulfosalicylic acids are known in analytical chemistry for forming high stability complexes with Fe^{3+} which are used in spectrophotometric analysis. However, unlike the aforementioned derivatives, salicylic and sulfosalicylic acids themselves showed weak or even adverse inhibiting effect for the tested alloys. This is because both acids also form stable complexes with Mg^{2+} ($logK_{Mg^{2+}}^{st}$ = 5.1 for sulfosalicylic acid)[98]. In this case, the positive effect of iron complexing is offset by accelerated Mg dissolution. Amino-, methyl-, nitro- and dinitro-derivatives of salicylic acid also form stable complexes with Fe^{3+} ($logK_{Fe^{3+}}^{st}$ = 18.13 for 3-methyl-, $logK_{Fe^{3+}}^{st}$ = 14.57 for 5-methyl-, $logK_{Fe^{3+}}^{st}$ = 14.19 for 3-nitrosalicylic acid [98-100]). The highest inhibiting effect of salicylic acid derivatives was found for highly corroding pure Mg (CP-Mg-220ppm and HP-

Mg-50ppm) and aluminium containing alloys AZ31, AZ91 and AM50. Related 4-hydroxybenzoic and 3,4-dihydroxibenzoic acids greatly accelerated dissolution of all Mg substrates because apart from chelating Fe^{3+}, they also form highly stable complexes with Mg^{2+} ($logK^{st}_{Mg^{2+}}$ = 9.84 for 3,4-dihydroxybenzoic acid) [99]. Salicylaldehide demonstrated high inhibiting efficiency for RE containing alloys, but should not be considered for the industrial use due to its toxicity to aquatic life.

A group of pyridinedicarboxylic acids, (2,6- , 2,5- , 2,3- and 3,4-PDCA) showed inhibiting efficiency >70% on average for all tested alloys and pure Mg. In PDCAs, the nitrogen protonation capability is greatly reduced due to enhanced deactivation of aromatic ring by second carboxylic group [101]. PDCAs are tridentate ligands forming rather strong chelates with Fe^{3+}, Fe^{2+} and weak complexes with Mg^{2+} (e.g. for 2,6-PDCA $logK^{st}_{Fe^{3+}}$ = 17.13, $logK^{st}_{Mg^{2+}}$ = 2.7 [102]). Given this, observed inhibiting effect is likely to be related with suppression of cathodic reaction on Fe-rich inclusions. Related pyridine monocarboxylic nicotinic and picolinic acids showed weaker inhibiting effect while quinaldic (quinolinecarboxylic) acid possesses high inhibiting effect similar to PDCAs.

EDTA exhibited slight inhibiting effect for highly corroding pure Mg (CP-Mg-220ppm and HP-Mg-50ppm). This is in line with previous reports that EDTA exhibits positive inhibiting effect for Mg-Ca$_{0.45}$ alloy [63] and recent report for pure Mg [74]. In contrast to pure Mg, corrosion of all the alloys was greatly accelerated. EDTA is one of the most widely used complexing agents and forms highly stable complexes with Fe^{2+} and Fe^{3+} along with Mg^{2+}, Zn^{2+}, Al^{3+}, etc. Similar effect of high corrosion acceleration was observed for a number of effective chelating agents: Tiron (pyrocatechol-3,5- disulphonate Na), nitrilotriacetic acid (NTA), N-(2-hydroxyethyl) ethylenediamine-N,N',N'-triacetic acid (HEDTA), Diethylenetriaminepenta acetic acid (DTPA), 1,2-Diaminocyclo-hexanetetra-acetic acid (DCTA). All of them are the chelating agents forming stable complexes with a number of cations and are used for chelate titration, masking or separation of cations. For the listed compounds, logKst$_{Fe3+}$ > 15 and logKst$_{Mg2+}$ > 5. Thus, just like in case of salicylic, sulfosalicylic and 3,4-dihydroxybenzoic acids, positive inhibiting effect due to iron complexation might be levelled out by the negative effect of complexing Mg^{2+} that accelerates Mg dissolution. Only at lower concentration, 0.001M EDTA or 0.0072M Tiron, inhibiting effect slightly improves, in some instances to positive values.

Benzoic acid showed the highest inhibiting efficiency to the alloys compared to its alkyl derivatives, like toluic, iso-propylbenzoic and tert-butylbenzoic acids. Interesting that amino- and nitro-derivatives of methyl-benzoic acid exhibited high inhibiting efficiency specifically to AZ31 alloy.

The amino-acids accelerated corrosion of all the alloys and some exhibited weak inhibiting effect for CP-Mg-220ppm and HP-Mg-50ppm pure magnesium with active iron impurities. Although the absolute values of inhibiting efficiency are different, the ranking order of individual amino-acids is very similar to that reported earlier for Mg–Al–Zn alloy [72]. Glycine, valine, alanine and leucine showed the lowest (negative) efficiency, while lysine, cysteine and threonine showed the highest inhibiting efficiency.

Saturated carboxylic acids (formic, acetic, propionic), di- and tri-carboxylic acids (oxalic, malonic, succinic, adipic, citric) and their hydroxy derivatives with one or more hydroxylic groups in alpha or other positions (glycolic, lactic, glyceric, tartaric, malic, gluconic) form medium stability complexes with Fe^{2+}/Fe^{3+} and hence can dampen the Fe/Fe^{2+}/Fe^{3+} redox cycle [98-100, 102]. E.g. logKst$_{Fe3+}$ = 3.1 for formic acid (and one of the iron-hydroxy-formiates has logKst$_{Fe3+}$ = 20.0), logKst$_{Fe3+}$ = 8.3 for acetic acid, logKst$_{Fe3+}$ = 3.4 for propionic acid) Most of these acids, tested in solutions adjusted to neutral pH, demonstrated high to medium inhibiting efficiency, especially to aluminium containing alloys and pure Mg. The prominent exception is the citric acid, which demonstrated enhanced hydrogen evolution for the alloys (but not for pure Mg with active Fe impurities). The reason is that citric acid, apart from iron complexes (logKst$_{Fe3+}$ > 11.5), also forms soluble complexes with Mg^{2+} ($logK^{st}_{Mg^{2+}}$ = 3.37) [99]. For the substrates where the effect of Fe on corrosion is the

strongest (CP-Mg-220ppm and HP-Mg-50ppm) the positive effect of iron complexation prevails over the negative effect of facilitating Mg dissolution which takes over in case of HP-Mg-51ppm and all six alloys.

Three unsaturated carboxylic acids were tested: citraconic, maleic and fumaric. The latter two are the *cis-* and *trans-* isomers of butenedioic acids. Interesting that while maleic acid has low inhibiting efficiency ranging for the alloys from -5% to 26% only, its *trans-* counterpart, fumaric acid, demonstrated much higher inhibiting efficiency (73% to 90%) for all (but ZE41) Mg materials. Although the stability constant of iron and magnesium fumarates were not found, multiple reports are available on synthesis of iron(II)-fumarate [103] and its use as iron-rich food supplement [104, 105] which is the indication of relative stability of Fe-fumarate.

2,2-bipyridyl and o-phenantroline also possess moderate inhibiting effect to most of the tested Mg materials. These two complexing agents are worth mentioning because they are the classical analytical reagents for colorimetric analysis of Fe^{2+} [106], although o-phenantroline also forms stable complexes with Fe^{3+} $logK^{st}_{Fe^{3+}}$ = 23.5 [102].

As it was previously explained, three main factors were considered at the pre-screening stage when selecting the compounds for hydrogen evolution tests:

    a) forms soluble complexes with Fe^{3+}/Fe^{2+}.

    b) forms sparingly soluble complexes with Mg^{2+}

    c) previously reported as corrosion inhibitor for one of the Mg alloys

Apart from Fe, detrimental influence of Cu and especially Ni on accelerating cathodic reaction of Mg is well known [107, 108]. Assuming that cathodic activity of Cu and Ni can be blocked by chelating mechanisms similar to that for Fe, several complexants specific to Cu (1,3,4-thiadiazole-2,5-dithiol - DMTD, benzotriazole - BTA) and Ni (dimethylglyoxime) were tested, but no pronounced inhibiting effect on corrosion of Mg alloys was revealed. This is likely because the impurity level of both Cu and Ni was low in the materials tested. Even EDS analysis of impurity particles did not reveal Cu and Ni enrichment, **Table 1** and **Table 4**. On the other hand, being the transition elements of first (3d) block, Fe, Ni and Cu possess similar properties reflecting on stability of formed chelates. E.g. for 2,6-pyridinedicarboxylic acid $logK^{st2}_{Fe^{3+}}$ = 17.13; $logK^{st2}_{Cu^{2+}}$ = 16.52; $logK^{st2}_{Ni^{2+}}$ = 13.50. For 2, 2'-bipyridyl $logK^{st3}_{Fe^{2+}}$ = 17.45; $logK^{st3}_{Cu^{2+}}$ = 17.08; $logK^{st3}_{Ni^{2+}}$ = 18.46. For salicylic acid $logK^{st2}_{Fe^{3+}}$ = 28.12; $logK^{st2}_{Cu^{2+}}$ = 18.28; $logK^{st2}_{Ni^{2+}}$ = 11.75 [102]. Thus, even in presence of higher amounts of Ni and Cu in Mg alloys, magnesium corrosion inhibitors dampening $Fe/Fe^{2+}/Fe^{3+}$ redox cycle are likely to have similar effect of Cu/Cu^{2+} and Ni/Ni^{2+} species.

Although the role of adsorption on inhibiting mechanism is not discussed in this paper because mechanistic understanding requires much more detailed investigation, we deem that adsorption layers formed on Mg or selectively on Fe-rich impurities might have a significant influence on inhibition by many of tested compounds. Research in this direction is planned.

As it was described above, correlation between inhibiting efficiency for HP-Mg-51ppm and HP-Mg-50ppm is lower (R^2 = 0.22) than that for CP-Mg-220ppm and HP-Mg-50ppm (R^2 = 0.50). The highest correlation of HP-Mg-51ppm inhibiting efficacy was found with Elektron 21 alloy (R^2 = 0.72). Inhibiting efficiency within the group of aluminium alloys also shows high correlation (average R^2 for three alloys is 0.86). The same applies to the group of three RE containing alloys (average R^2 for three alloys is 0.70), while correlation between the groups of Al- and RE-containing alloys is lower (R^2 = 0.56). Summarizing, corrosion and consequently inhibition of pure Mg greatly depends on the impurity level and distribution of Fe in impurity particles. Application of corrosion inhibitor found to be effective for RE-containing Mg alloy will not necessarily be successful for Al-containing Mg alloy, while use of the same inhibitor within the same group of Mg alloys is more likely to yield positive effect.

3.4 Inhibitors ranking

Fifteen the most efficient inhibitors for three groups of Mg alloys are ranked in **Table 5**. Sodium salts of pyridine-dicarboxylic acids (especially 2,5- and 2,6-PDCA) and Na salts of several derivatives of salicylic acids (3,5-dinitrosalicylate, 3-nitrosalicylate, 4- and 5-aminosalicylate and 3- and 5-methylsalicylate) possess high inhibiting efficiency for the entire range of tested Mg materials. It is comparable or even higher than the efficiency of carcinogenic chromate - Cr(VI) - traditionally used by corrosion protection strategies for Mg alloys. This is an encouraging outcome, especially in view of the shortly approaching Sunset Date (21-09-2017) for the use of chromate containing treatments and pigments. Even though the ban to use Cr(VI) compounds in aerospace industry implied by REACH authorisation list (Annex XIV) is likely to be postponed until year 2024 [109], the use of Cr(VI) will eventually be prohibited for all the industries. This makes finding new corrosion inhibitors suitable for industrial applications timely and highly relevant.

Beside the salts of pyridinedicarboxylic and salicylic acids, the differences in the list of best 15 inhibitors for each group of alloys are rather significant. On the other hand, quinaldates and nitrate (both equivocally carcinogenic) along with fumarates and nitrobarbiturates demonstrated high inhibiting efficiency to a number of tested alloys.

Table 5. Selection of 15 the most efficient corrosion inhibitors for pure Mg. Toxic, carcinogenic and harmful for environment substances are marked. Question mark means that mutagenic or carcinogenic effects are suspected.

	CP-Mg-220ppm		HP-Mg-51 ppm		HP-Mg-50 ppm	
1	Salicylaldehide	98	2, 5-Pyridinedicarboxylate Na	92	2,5-Pyridinedicarboxylate Na	99
2	3-Methylsalicylate Na	97	Folate Na	89	2,6-Pyridinedicarboxylate Na	99
3	KNO_3 ?	97	Na_2CrO_4	85	2,3-Pyridinedicarboxylate Na	98
4	8-Hydroxyquinoline ?	95	3,5-Dinitrosalicylate Na	81	3,4-Pyridinedicarboxylate Na	97
5	KCN	94	2,6-Pyridinedicarboxylate Na	75	KNO_3 ?	97
6	Dodecylbenzene Sulfonate Na	93	Fumarate Na	73	2-Hydroxy-1,4-Naphtoquinone	97
7	Na_3PO_4	93	Quinaldate Na ?	70	Fumarate Na	95
8	Salicylate Na	92	2,3-Pyridinedicarboxylate Na	70	3-MethylSalicylate Na	94
9	$Ce(NO_3)_3$	92	3,4-Pyridinedicarboxylate Na	64	4-Isopropylbenzoate Na	94
10	2,6-Pyridinedicarboxylate Na	90	2-Thenoyltrifluoroacetone	63	5-MethylSalicylate Na	93
11	$La(NO_3)_3$	88	5-Methylsalicylate Na	61	NaF	93
12	5-Aminosalicylate Na	86	4-Isopropylbenzoate Na	51	Succinate Na	93
13	Oxalate Na	86	2-Hydroxy-1,4Naphtoquinone	48	Diglycolate Na	93
14	Diglycolate Na	86	Benzoate Na	48	Oxalate Na	93
15	Thiosalicylate Na	86	N-Lauroylsarcosine Na	47	$Ce(NO_3)_3$	90
Cr(VI) ranked	**50**	61	**3**	85	**62**	56

	WE43		ZE41		Elektron 21	
1	Salicylaldehide ⚠☠	95	KNO$_3$ [?]	95	Fumarate Na	90
2	KNO$_3$ [?]	88	NaF ⚠	75	KNO$_2$ ⚠☠	89
3	Fumarate Na	87	3-Methylsalicylate Na	75	2, 5-Pyridinedicarboxylate Na	83
4	2,5-Pyridinedicarboxylate Na	83	2,6-Pyridinedicarboxylate Na	71	3,5-Dinitrosalicylate Na	82
5	Na$_2$CrO$_4$ ⚠☢☠	80	N-Lauroylsarcosine Na ⚠	70	Salicylaldehide ⚠☢☠	82
6	5-Methylsalicylate Na	76	Na$_2$SO$_4$	68	3,4-Pyridinedicarboxylate Na	81
7	2,6-Pyridinedicarboxylate Na	73	5-Aminosalicylate Na	66	Folate Na	77
8	3,4-Pyridinedicarboxylate Na	71	Malate Na	63	5-Methylsalicylate Na	76
9	5-Nitrobarbituriate Na	71	Ce(NO$_3$)$_3$ ⚠	62	KNO$_3$ [?]	75
10	KNO$_2$ ⚠☠	70	Diglycolate Na	60	Quinaldate Na [?]	70
11	3,5-Dinitrosalicylate Na	70	5-Methylsalicylate Na	59	2,6-Pyridinedicarboxylate Na	69
12	3-Nitrosalicylate Na	66	Glycolate Na	59	Pyrazine	69
13	Oleiate Na	64	3,4-Pyridinedicarboxylate Na	57	Oleate Na	65
14	Quinaldate Na [?]	62	4-Aminosalicylate Na	57	N-Lauroylsarcosine Na ☠	64
15	Lactobionate Na	59	Lactobionate Na	55	Ce(NO$_3$)$_3$ ⚠	62
Cr(VI) ranked	5	80	90	-39	16	62

	AZ31		AZ91		AM50	
1	KNO$_2$ ⚠☠	95	Na$_2$CrO$_4$ ⚠☢☠	88	KNO$_3$ [?]	87
2	Na$_2$CrO$_4$ ⚠☢☠	94	3,5-Dinitrosalicylate Na	86	Na$_2$CrO$_4$ ⚠☢☠	82
3	Fumarate Na	90	Fumarate Na	83	3,5-Dinitrosalicylate Na	81
4	2-Hydroxy-1,4-Naphtoquinone	90	KNO$_2$ ⚠☠	82	Fumarate Na	80
5	5-Methyl-2-nitrobenzoate Na	90	5-Aminosalicylate Na	80	KNO$_2$ ⚠☠	79
6	Quinaldate Na [?]	86	Quinaldate Na [?]	74	5-Aminosalicylate Na	77
7	KNO$_3$ [?]	86	3-Nitrosalicylate Na	74	Quinaldate Na [?]	77
8	2, 5-Pyridinedicarboxylate Na	84	Ce(NO$_3$)$_3$ ⚠	73	5-Nitrobarbiturate Na	74
9	4-Isopropylbenzoate Na	84	KNO$_3$ [?]	71	3,4-Pyridinedicarboxylate Na	74
10	5-Aminosalicylate Na	83	5-Nitrobarbiturate Na	71	2, 5- Pyridinedicarboxylicate Na	70
11	Ce(NO$_3$)$_3$ ⚠	83	2-Thenoyltrifluoroacetone	71	Benzoate Na	70
12	3,4-Pyridinedicarboxylate Na	82	2, 5-Pyridinedicarboxylate Na	68	2,6-Pyridinedicarboxylate Na	69
13	2,6-Pyridinedicarboxylate Na	79	3,4-Pyridinedicarboxylate Na	67	3-Nitrosalicyliate Na	68
14	3-Methylsalicylate Na	78	Thiosalicylate Na	67	3-Methylsalicylate Na	66
15	Formate Na	78	Dodecylbenzene Sulfonate Na	67	Pyrazine	61
Cr(VI) ranked	2	94	1	88	2	82

Some of presented values of inhibiting efficiency correlate well with earlier reported data [12, 13, 16, 40], while in some cases lower inhibiting efficiently was found. This should not be considered as a disturbing contradiction for several reasons. Inhibiting efficiency greatly depends on the composition and impurities present in any particular Mg material. Striking difference of corrosion behaviour and inhibition of two high purity Mg, containing slightly different amount of impurities (HP-Mg-50ppm and HP-Mg-51ppm), is a vivid example, see **part 3.2**. Besides, a compound possessing high inhibiting efficiency to one specific alloy might accelerate dissolution of another alloy. **Table** 3 is full of such examples, e.g. Na salts of glycolic, diglycolic, oxalic and tartaric acids exhibit medium to high inhibiting efficiency to Al-containing Mg alloys but greatly accelerate corrosion of E21. Concentration of the inhibitor and duration of the immersion test before the cut-off measurement for calculating the inhibiting efficiency also greatly influences the inhibiting efficiency value. All in all, chemical composition of the alloys including impurities, corrosion medium, concentration of the inhibitor, (initial) pH and immersion time need to be considered together with inhibiting efficiency for the full-fledged comparison.

Albeit, comparison is not always feasible, the database presented in this work ranks Mg corrosion inhibitors tested in the same conditions for a number of industrially important alloys. We consider this as a starting point for understanding the particularities of corrosion inhibition of each specific alloy and for in depth studies of inhibiting mechanisms of the most effective inhibitors. Naturally, varying concentration of inhibitors as well as exposure time and conditions may and will result in different inhibiting efficiencies. Another direction is the development of the most suitable and cost-effective ways of incorporating new inhibitors into the chemical conversion coatings, primers (including epoxy and silane based) and paints for impairing them with active corrosion protection. Again note, that behaviour of the same inhibitor when in contact with a bare alloy or dispersed in a coating may also result in different inhibiting mechanism and hence different inhibiting efficiency as it was shown for the aluminium alloy 2024 [110].

3.4 Where to use Mg dissolution promoters?

A number of tested organic compounds have shown acceleration of Mg dissolution, in some cases above 500 %. In spite of seemingly negative results, there substances are also likely to find extended application, for example as electrolyte additives for Mg primary batteries [70, 73, 111]. Suppression of Mg self-corrosion, proposed here via complexing iron impurities, is one of the main requirements for primary battery applications. When supported by moderate complexation of Mg^{2+} (to prevent formation of blocking precipitate of $Mg(OH)_2$ on the battery anode) such complexing agents boost performance of Mg-air batteries. Only the complexing agents that form soluble complexes with Mg allow for elevated voltage of Mg batteries. The example of such species are Na Salicylate, Tiron, Na Nitrilotriacetate, Na-EDTA [70, 73, 111] and sodium citrate [112]. Compounds that form sparingly soluble species with Mg, like sodium oxalate and sodium dodecylbenzenesulfonate do not improve battery performance because the anode surface rapidly becomes blocked [70, 73]. Several more applications for Mg dissolution promoters are currently being explored and will be reported later.

The data presented in **Table 3** can also be used to shed some light on the behaviour of bioresorbable implants. Whole blood or its serum contains several tens of compounds that can be considered Mg or Fe complexing agents. Their low concentrations might be compensated by the high number of such compounds constituting the bio-liquids. Meanwhile, only a fraction of them is included in the simulated body fluid solutions used as testing medium for studying dissolution of Mg parts. SBF or DMEM only partly take into account the complexity of the chemical composition of blood and serum that contain multiple Fe and Mg complexing agents. Very limited variety of vitamins and drugs tested in this work has shown their significant

influence on Mg dissolution that varies from alloy to alloy. E.g. folic acid (strong Fe complexing agent) demonstrated inhibiting effect for most of the alloys. The effect of ascorbic acid varies depending on the alloy and ranges from +87% for HP-Mg-50ppm to -401% for Elektron 21 alloy. Similar effect but with narrower variation of inhibiting efficiency was observed for Glucose. Tris, D-panthenol, streptomycin and penicillin (two latter are added to DMEM for preventing bacteria growth) revealed marked corrosion acceleration effect on tested Mg alloys. Detailed study on influence of individual components of bio-fluid on degradation rate of Mg alloys is needed. Including several more key organic compounds to the simulated body fluids used for Mg testing and taking into account corrosion acceleration by media components like tris, streptomycin and penicillin, might improve general understanding and allow for better than reported [113] matching of *in-vitro* and *in-vivo* test results of Mg degradation.

4. Conclusions

151 individual chemical compounds were tested and their ability to inhibit corrosion was ranked for pure Mg and AZ31, AZ91, AM50, WE43, ZE41 and Elektron 21 alloys. A number of new corrosion inhibitors have been identified with the inhibiting efficiency comparable or even exceeding that of carcinogenic Cr(VI). The sodium salts of derivatives of pyridinedicarboxylic and salicylic acids are the most efficient and universal when it comes to inhibiting corrosion of pure Mg, Al- or RE-containing alloys. Majority of other tested inhibitors are not universal, i.e. the inhibitor effective for ZE41 alloy might not necessarily possess similar inhibiting efficiency for AZ31 alloy. However, good correlation is observed between the inhibiting efficiency within groups of Al- or RE containing alloys and pure Mg.

The values of inhibiting efficiency presented in this work varied in a wide range with varying concentration of the inhibitor. Among other factors, pH buffering effect that inhibitors might possess, is responsible for this. Traditional effects were observed such as passivation/precipitation due to formation of sparingly soluble Mg complexes on Mg surface. Relatively new general trend was also emphasized that compounds forming highly stable complexes with Fe^{3+}/Fe^{2+} are efficient inhibitors of Mg corrosion. The effect is especially high for the materials including Fe-rich impurities acting as local cathodes initiating microgalvanic corrosion. On the other hand, the effect is low or even negative, if substances forming Fe^{3+}/Fe^{2+} chelates also bind Mg^{2+} in soluble complexes. These effects are important for developing new strategies for corrosion inhibition of Mg alloys but also for the development of electrolytes for primary Mg-air batteries and for understanding Mg degradation in bio environments.

References

[1] Kurze P. 7.1 Surface Treatments and Protection. In: Friedrich HF, Mordike BL, editors. Magnesium Technology Metallurgy, Design Data, Applications: Springer; 2006. p. 431-67.

[2] Höche D, Nowak A, Schillings T. Surface cleaning and pre-conditioning surface treatments to improve the corrosion resistance of magnesium (Mg) alloys. In: Song GL, editor. Corrosion prevention of Magnesium: Woodhead Publishing; 2012.

[3] Supplit R, Koch T, Schubert U. Evaluation of the anti-corrosive effect of acid pickling and sol–gel coating on magnesium AZ31 alloy. Corrosion Science 2007;49:3015-23.

[4] Nwaogu UC, Blawert C, Scharnagl N, Dietzel W, Kainer KU. Influence of inorganic acid pickling on the corrosion resistance of magnesium alloy AZ31 sheet. Corrosion Science 2009;51:2544-56.

[5] Nwaogu UC, Blawert C, Scharnagl N, Dietzel W, Kainer KU. Effects of organic acid pickling on the corrosion resistance of magnesium alloy AZ31 sheet. Corrosion Science 2010;52:2143-54.

[6] Hillis J. 7.2 Corrosion. In: Friedrich HF, Mordike BL, editors. Magnesium Technology Merallurgy, Design Data, Applications: Springer; 2006. p. 469-98.

[7] X.-B. Chen, M.A. Easton, N. Birbilis, Yang H-Y, Abbott TB. Corrosion -resistant coatings for magnesium (Mg) alloys. In: G.-L. S, editor. Corrosion prevention of magnesium alloys: Woodhead Publishing; 2013. p. 282-312.

[8] Pommiers S, Frayret J, Castetbon A, Potin-Gautier M. Alternative conversion coatings to chromate for the protection of magnesium alloys. Corrosion Science 2014;84:135-46.

[9] Hughes AE, Mol JMC, Zheludkevich ML, Buchheit RG. Active protective coatings: new-generation coatings for metals: Springer; 2016.

[10] Lamaka S.V., Lourenço M. M., Ivanov D. K., Zheludkevich M.L., Ferreira M.G.S., T. H. Fault-tolerant composite protective coating for WE43 magnesium alloy. Proceedings of the IMA 2014 World Annual Magnesium Conference2014. p. 116-22.

[11] Guo X-P, Song G-L, Hu J-Y, Huang D-B. Corrosion inhibitors of magnesium (Mg) alloys. In: Song G-L, editor. Corrosion prevention of magnesium alloys: Woodhead Publishing; 2013. p. 61-84.

[12] D. Huang YT, G. Song, X. Guo. Inhibition Effects of Pyrazine and Piperazine on the Corrosion of Mg-10Gd-3Y-0.5Zr Alloy in an Ethylene Glycol Solution. American Journal of Analytical Chemistry 2013;4:36-8.

[13] Frignani A, Grassi V, Zanotto F, Zucchi F. Inhibition of AZ31 Mg alloy corrosion by anionic surfactants. Corrosion Science 2012;63:29-39.

[14] Gao H, Li Q, Dai Y, Luo F, Zhang HX. High efficiency corrosion inhibitor 8-hydroxyquinoline and its synergistic effect with sodium dodecylbenzenesulphonate on AZ91D magnesium alloy. Corrosion Science 2010;52:1603-9.

[15] Williams G, Grace R, Woods RM. Inhibition of the Localized Corrosion of Mg Alloy AZ31 in Chloride Containing Electrolyte. CORROSION 2015;71:184-98.

[16] Semiletov AM. Metals passivation by aqueous solutions of organic acids and trialkoxysilanes, In Russian: Moscow State University, PhD; 2016.

[17] Lamaka SV, Höche D, Petrauskas RP, Blawert C, Zheludkevich ML. A new concept for corrosion inhibition of magnesium: Suppression of iron re-deposition. Electrochemistry Communications 2016;62:5-8.

[18] Dang N, Wei YH, Hou LF, Li YG, Guo CL. Investigation of the inhibition effect of the environmentally friendly inhibitor sodium alginate on magnesium alloy in sodium chloride solution. Materials and Corrosion 2015;66:1354-62.

[19] Hu J, Zeng D, Zhang Z, Shi T, Song G-L, Guo X. 2-Hydroxy-4-methoxy-acetophenone as an environment-friendly corrosion inhibitor for AZ91D magnesium alloy. Corrosion Science 2013;74:35-43.

[20] Hu J, Huang D, Zhang G, Song G-L, Guo X. Research on the inhibition mechanism of tetraphenylporphyrin on AZ91D magnesium alloy. Corrosion Science 2012;63:367-78.

[21] Hou L, Dang N, Yang H, Liu B, Li Y, Wei Y, et al. A Combined Inhibiting Effect of Sodium Alginate and Sodium Phosphate on the Corrosion of Magnesium Alloy AZ31 in NaCl Solution. Journal of The Electrochemical Society 2016;163:C486-C94.

[22] Thirugnanaselvi S, Kuttirani S, Emelda AR. Effect of Schiff base as corrosion inhibitor on AZ31 magnesium alloy in hydrochloric acid solution. Transactions of Nonferrous Metals Society of China 2014;24:1969-77.

[23] Dinodi N, Shetty AN. Alkyl carboxylates as efficient and green inhibitors of magnesium alloy ZE41 corrosion in aqueous salt solution. Corrosion Science 2014;85:411-27.

[24] Chen LD, Nørskov JK, Luntz AC. Theoretical Limits to the Anode Potential in Aqueous Mg–Air Batteries. The Journal of Physical Chemistry C 2015;119:19660-7.

[25] Taylor CD. Modeling Corrosion, Atom by Atom. The Electrochemical Society Interface 2014;23:59-64.

[26] Francis MF, Taylor CD. First-principles insights into the structure of the incipient magnesium oxide and its instability to decomposition: Oxygen chemisorption to Mg(0001) and thermodynamic stability. Physical Review B 2013;87:075450.

[27] Chen XB, Birbilis N, Abbott TB. Review of Corrosion-Resistant Conversion Coatings for Magnesium and Its Alloys. CORROSION 2011;67:035005-1--16.

[28] Zhao M, Wu S, An P, Luo J. Influence of surface pretreatment on the chromium-free conversion coating of magnesium alloy. Materials Chemistry and Physics 2007;103:475-83.

[29] Chiu KY, Wong MH, Cheng FT, Man HC. Characterization and corrosion studies of fluoride conversion coating on degradable Mg implants. Surface and Coatings Technology 2007;202:590-8.

[30] Han Z, Chen H, Zhou S. Dissociation and diffusion of hydrogen on defect-free and vacancy defective Mg (0001) surfaces: A density functional theory study. Applied Surface Science 2017;394:371-7.

[31] Harvey TG, Hardin SG, Hughes AE, Muster TH, White PA, Markley TA, et al. The effect of inhibitor structure on the corrosion of AA2024 and AA7075. Corrosion Science 2011;53:2184-90.

[32] Winkler DA, Breedon M, White P, Hughes AE, Sapper ED, Cole I. Using high throughput experimental data and in silico models to discover alternatives to toxic chromate corrosion inhibitors. Corrosion Science 2016;106:229-35.

[33] Winkler DA, Breedon M, Hughes AE, Burden FR, Barnard AS, Harvey TG, et al. Towards chromate-free corrosion inhibitors: structure-property models for organic alternatives. Green Chemistry 2014;16:3349-57.

[34] Muster TH, Sullivan H, Lau D, Alexander DLJ, Sherman N, Garcia SJ, et al. A combinatorial matrix of rare earth chloride mixtures as corrosion inhibitors of AA2024-T3: Optimisation using potentiodynamic polarisation and EIS. Electrochimica Acta 2012;67:95-103.

[35] Zheludkevich ML, Yasakau KA, Poznyak SK, Ferreira MGS. Triazole and thiazole derivatives as corrosion inhibitors for AA2024 aluminium alloy. Corrosion Science 2005;47:3368-83.

[36] Yasakau KA, Zheludkevich ML, Lamaka SV, Ferreira MGS. Mechanism of corrosion inhibition of AA2024 by rare-earth compounds. Journal of Physical Chemistry B 2006;110:5515-28.

[37] Höche D, Blawert C, Lamaka SV, Scharnagl N, Mendis C, Zheludkevich ML. The effect of iron re-deposition on the corrosion of impurity-containing magnesium. Physical chemistry chemical physics : PCCP 2016;18:1279-91.

[38] King AD, Birbilis N, Scully JR. Accurate Electrochemical Measurement of Magnesium Corrosion Rates; a Combined Impedance, Mass-Loss and Hydrogen Collection Study. Electrochimica Acta 2014;121:394-406.

[39] Parasuraman S. Toxicological screening. Journal of Pharmacology and Pharmacotherapeutics 2011;2:74-9.

[40] Williams G, McMurray HN, Grace R. Inhibition of magnesium localised corrosion in chloride containing electrolyte. Electrochimica Acta 2010;55:7824-33.

[41] Richey FW, McCloskey BD, Luntz AC. Mg Anode Corrosion in Aqueous Electrolytes and Implications for Mg-Air Batteries. Journal of The Electrochemical Society 2016;163:A958-A63.

[42] S.Sathyanarayana NM. A new magnesium - air cell for long-life applications. J Appl Electrochem 1981;11:33-9.

[43] Wang SY, Li Q, Zhong XK, Li LQ, Chen FN, Luo F, et al. Effects of NO−3in NaCl solution on corrosion protection of AZ91D magnesium alloy coated with silane films. Transactions of the IMF 2012;90:78-85.

[44] Song G, StJohn DH. Corrosion of magnesium alloys in commercial engine coolants. Materials and Corrosion 2005;56:15-23.

[45] Karavai OV, Bastos AC, Zheludkevich ML, Taryba MG, Lamaka SV, Ferreira MGS. Localized electrochemical study of corrosion inhibition in microdefects on coated AZ31 magnesium alloy. Electrochimica Acta 2010;55:5401-6.

[46] Kartsonakis IA, Stanciu SG, Matei AA, Karaxi EK, Hristu R, Karantonis A, et al. Evaluation of the protective ability of typical corrosion inhibitors for magnesium alloys towards the Mg ZK30 variant. Corrosion Science 2015;100:194-208.

[47] Zeng R-C, Hu Y, Guan S-K, Cui H-Z, Han E-H. Corrosion of magnesium alloy AZ31: The influence of bicarbonate, sulphate, hydrogen phosphate and dihydrogen phosphate ions in saline solution. Corrosion Science 2014;86:171-82.

[48] http://www.sciencelab.com/msds.php?msdsId=9924691.

[49] Li L, Lei L. Inhibition of molybdate salt on dissolution of magnesium alloys in phosphoric acid. Surface Technology 2007;36:16-8.

[50] Yong Z, Zhu J, Qiu C, Liu Y. Molybdate/phosphate composite conversion coating on magnesium alloy surface for corrosion protection. Applied Surface Science 2008;255:1672-80.

[51] Yang KH, Ger MD, Hwu WH, Sung Y, Liu YC. Study of vanadium-based chemical conversion coating on the corrosion resistance of magnesium alloy. Materials Chemistry and Physics 2007;101:480-5.

[52] Hamdy AS, Doench I, Möhwald H. Vanadia-based coatings of self-repairing functionality for advanced magnesium Elektron ZE41 Mg–Zn–rare earth alloy. Surface and Coatings Technology 2012;206:3686-92.

[53] Lin J, Battocchi D, Bierwagen GP. Inhibitors for prolonging corrosion protection of Mg-rich primer on Al alloy 2024-T3. J Coat Technol Res 2017:1-8.

[54] Li L, Pan F, Lei J. Environmental Friendly Corrosion Inhibitors for Mg Alloys. In: F.Czerwinski, editor. In Mg Alloys - Corrosion and Surface Treatments: InTech; 2011.

[55] Lamaka SV, Zheludkevich ML, Yasakau KA, Montemor MF, Ferreira MGS. High effective organic corrosion inhibitors for 2024 aluminium alloy. Electrochimica Acta 2007;52:7231-47.

[56] Lamaka SV, Knörnschild G, Snihirova DV, Taryba MG, Zheludkevich ML, Ferreira MGS. Complex anticorrosion coating for ZK30 magnesium alloy. Electrochimica Acta 2009;55:131-41.

[57] Galio AF, Lamaka SV, Zheludkevich ML, Dick LFP, Müller IL, Ferreira MGS. Inhibitor-doped sol–gel coatings for corrosion protection of magnesium alloy AZ31. Surface and Coatings Technology 2010;204:1479-86.

[58] Gnedenkov AS, Sinebryukhov SL, Mashtalyar DV, Gnedenkov SV. Localized corrosion of the Mg alloys with inhibitor-containing coatings: SVET and SIET studies. Corrosion Science 2016;102:269-78.

[59] Slavcheva E, Schmitt G. Screening of new corrosion inhibitors via electrochemical noise analysis. Materials and Corrosion 2002;53:647-55.

[60] S.V. L, D. H, M.L. Z. Group of corrosion inhibitors for magnesium and magnesium alloys, EP16184196. 2016.

[61] Guo X, An M, Yang P, Li H, Su C. Effects of benzotriazole on anodized film formed on AZ31B magnesium alloy in environmental-friendly electrolyte. Journal of Alloys and Compounds 2009;482:487-97.

[62] Wang J-L, Ke C, Pohl K, Birbilis N, Chen X-B. The Unexpected Role of Benzotriazole in Mitigating Magnesium Alloy Corrosion: A Nucleating Agent for Crystalline Nanostructured Magnesium Hydroxide Film. Journal of The Electrochemical Society 2015;162:C403-C11.

[63] Ostanina TN, Rudoi VM, Ovsyannikova AN, Malkov VB. Magnesium alloys spontaneous dissolution features under external anodic polarization in presence of inhibitors. Russ J Electrochem 2010;46:707-13.

[64] K.Fukumura, Shiraishi T. Surface-treating agent for magnesium-based part and method of surface treatment. US 6569264 B1. 2003.

[65] K.Fukumura, Y.Yu, M.Kajimoto, H.Hama, T.Hamauzu, H.Yagi. Rust preventive for magnesium and/or magnesium alloy. US20070080319A1, EP1683894A1. 2007.

[66] J.L. Lei, L.J. Li, H.S. Yu, M.L.Chen, S.T. Zhang, Pan FS. Inhibition of hexamethylenetetramine on corrosion of magnesium alloy in simulated coolant. ChemRes and Appl 2008;20:461-4.

[67] Ivanou DK, Yasakau KA, Kallip S, Lisenkov AD, Starykevich M, Lamaka SV, et al. Active corrosion protection coating for a ZE41 magnesium alloy created by combining PEO and sol–gel techniques. RSC Advances 2016;6:12553-60.

[68] Lamaka S.V., Hoeche D., Blawert C., M.L.. Z. Corrosion Inhibitor Composition for Magnesium or Magnesium Alloys, EP15189674. 2015.

[69] Lamaka SV, Höche D, Blawert C, Zheludkevich ML. Corrosion Inhibitor Composition for Magnesium or Magnesium Alloys. In: HZG, editor. European Patent Office EP151896743. EU: DE; 2015.

[70] Hoeche D, Lamaka SV, Zheludkevich ML. Electrolyte additives for magneisum air batteries, 16187152.0. 2016.

[71] Cui X, Li Y, Li Q, Jin G, Ding M, Wang F. Influence of phytic acid concentration on performance of phytic acid conversion coatings on the AZ91D magnesium alloy. Materials Chemistry and Physics 2008;111:503-7.

[72] Helal NH, Badawy WA. Environmentally safe corrosion inhibition of Mg–Al–Zn alloy in chloride free neutral solutions by amino acids. Electrochimica Acta 2011;56:6581-7.

[73] Höche D, Lamaka SV, Vaghefinazari B, T.Braun, Petrauskas RP, M.Fichtner, et al. High power primary Mg-air battery via electrolyte additives. Submitted 2017.

[74] McMurray HN, Williams G, Michailidou E. The role of transition metal (Re)plating in the cathodic activation of corroding magnesium. Eurocorr 2016. Montpellier, France2016. p. Keynote lecture.

[75] Lamaka SV, Xue HB, Meis NNAH, Esteves ACC, Ferreira MGS. Fault-tolerant hybrid epoxy-silane coating for corrosion protection of magnesium alloy AZ31. Progress in Organic Coatings 2015;80:98-105.

[76] Muster TH, Hughes AE, Furman SA, Harvey T, Sherman N, Hardin S, et al. A rapid screening multi-electrode method for the evaluation of corrosion inhibitors. Electrochimica Acta 2009;54:3402-11.

[77] Lunder O, Nordien JH, Nisancioglu K. Corrosion resistance of cast Mg-Al alloys. Corrosion Reviews 1997;15:439-70.

[78] Yang L, Zhou X, Liang S-M, Schmid-Fetzer R, Fan Z, Scamans G, et al. Effect of traces of silicon on the formation of Fe-rich particles in pure magnesium and the corrosion susceptibility of magnesium. Journal of Alloys and Compounds 2015;619:396-400.

[79] Song GL, Atrens A. Corrosion Mechanisms of Magnesium Alloys. Advanced Engineering Materials 1999;1:11-33.

[80] Prasad A, Uggowitzer PJ, Shi Z, Atrens A. Production of High Purity Magnesium Alloys by Melt Purification with Zr. Advanced Engineering Materials 2012;14:477-90.

[81] Gandel DS, Easton MA, Gibson MA, Abbott T, Birbilis N. The influence of zirconium additions on the corrosion of magnesium. Corrosion Science 2014;81:27-35.

[82] Eliezer D, Uzan P, Aghion E. Effect of second phases on the corrosion behavior of magnesium alloys. Trans Tech Publ. p. 857-66.

[83] Zeng R-c, Zhang J, Huang W-j, Dietzel W, Kainer KU, Blawert C, et al. Review of studies on corrosion of magnesium alloys. Transactions of Nonferrous Metals Society of China 2006;16:s763-s71.

[84] Song G, Atrens A. Understanding Magnesium Corrosion—A Framework for Improved Alloy Performance. Advanced Engineering Materials 2003;5:837-58.

[85] Mayilvel Dinesh M, Saminathan K, Selvam M, Srither SR, Rajendran V, Kaler KVIS. Water soluble graphene as electrolyte additive in magnesium-air battery system. Journal of Power Sources 2015;276:32-8.

[86] Aldykewicz AJ, Isaacs HS, Davenport AJ. The Investigation of Cerium as a Cathodic Inhibitor for Aluminum-Copper Alloys. Journal of The Electrochemical Society 1995;142:3342-50.

[87] Aballe A, Bethencourt M, Botana FJ, Marcos M. CeCl3 and LaCl3 binary solutions as environment-friendly corrosion inhibitors of AA5083 Al–Mg alloy in NaCl solutions. Journal of Alloys and Compounds 2001;323–324:855-8.

[88] Paussa L, Andreatta F, De Felicis D, Bemporad E, Fedrizzi L. Investigation of AA2024-T3 surfaces modified by cerium compounds: A localized approach. Corrosion Science 2014;78:215-22.

[89] Cui X, Yang Y, Liu E, Jin G, Zhong J, Li Q. Corrosion behaviors in physiological solution of cerium conversion coatings on AZ31 magnesium alloy. Applied Surface Science 2011;257:9703-9.

[90] Montemor MF, Simões AM, Ferreira MGS, Carmezim MJ. Composition and corrosion resistance of cerium conversion films on the AZ31 magnesium alloy and its relation to the salt anion. Applied Surface Science 2008;254:1806-14.

[91] Rudd AL, Breslin CB, Mansfeld F. The corrosion protection afforded by rare earth conversion coatings applied to magnesium. Corrosion Science 2000;42:275-88.

[92] Mohedano M, Blawert C, Zheludkevich ML. Silicate-based Plasma Electrolytic Oxidation (PEO) coatings with incorporated CeO2 particles on AM50 magnesium alloy. Materials & Design 2015;86:735-44.

[93] Yoe JH, Hall RT. A Study of 7-Iodo-8-hydroxyquinoline-5-sulfonic Acid as a Reagent for the Colorimetric Determination of Ferric Iron1. Journal of the American Chemical Society 1937;59:872-9.

[94] Przeszlakowski S, Habrat E. Extraction of iron(III) from aqueous solution with mixtures of Aliquat 336 and ferron in chloroform. Analyst 1982;107:1320-9.

[95] Fleck HR, Ward AM. The determination of metals by means of 8-hydroxyquinoline. Part I. The effect of pH on the precipitation of magnesium, zinc, cobalt, nickel, copper and molybdenum from acetate solutions. Analyst 1933;58:388-95.

[96] Serdechnova M, Ivanov VL, Domingues MRM, Evtuguin DV, Ferreira MGS, Zheludkevich ML. Photodegradation of 2-mercaptobenzothiazole and 1,2,3-benzotriazole corrosion inhibitors in aqueous solutions and organic solvents. Physical Chemistry Chemical Physics 2014;16:25152-60.

[97] Berlin A, Robinson RJ. THermogravimetric determination of magnesium, potassium and lead by precipitation with dilituric acid. Analytic aChimica Acta 1961;24:224-34.

[98] Martell AE, Smith RM. Critical Stability Constants: Second Supplement, V. 6: Springer Science & Business Media; 1989.

[99] Martell AE, Smith RM. Critical Stability Constants, Other organic ligands, V. 3. New York: Springer; 1977.

[100] Martell AE, Smith RM. Critical Stability Constants: First Supplement, V. 5: Springer Science & Business Media; 1982.

[101] Ranganathan S, Prince AAM, Raghavan PS, Gopalan R, Srinivasan MP, Narasimhan SV. Kinetics of Dissolution of Magnetite in PDCA Based Formulations. Journal of Nuclear Science and Technology 1997;34:810-6.

[102] Dean JA. Lange's chemistry handbook. 15 ed: McGraw-Hill, New York; 1999.

[103] Kapor AJ, Nikolić LB, Nikolić VD, Stanković MZ, Cakić MD, Ilić DP, et al. THE SYNTHESIS AND CHARACTERIZATION OF IRON(II) FUMARATE AND ITS INCLUSION COMPLEXES WITH CYCLODEXTRINS. Advanced Technologies 2012;1:7-15.

[104] Geltman PL, Hironaka LK, Mehta SD, Padilla P, Rodrigues P, Meyers AF, et al. Iron Supplementation of Low-Income Infants: A Randomized Clinical Trial of Adherence with Ferrous Fumarate Sprinkles Versus Ferrous Sulfate Drops. The Journal of Pediatrics 2009;154:738-43.e1.

[105] Liu T-C, Lin S-F, Chang C-S, Yang W-C, Chen T-P. Comparison of a Combination Ferrous Fumarate Product and a Polysaccharide Iron complex as Oral Treatments of Iron Deficiency Anemia: A Taiwanese Study. International Journal of Hematology 2004;80:416.

[106] Charlot G. Les Méthodes de la chimie analytique : Analyse quantitative minérale. : Masson; 1960.

[107] Makar G, Kruger J. Corrosion of magnesium. International Materials Reviews 1993;38:138-53.

[108] Blawert C, Fechner D, Höche D, Heitmann V, Dietzel W, Kainer KU, et al. Magnesium secondary alloys: Alloy design for magnesium alloys with improved tolerance limits against impurities. Corrosion Science 2010;52:2452-68.

[109] REACH. http://www.jonesdayreach.com/SitePages/Home.aspx.

[110] Snihirova D, Lamaka SV, Taheri P, Mol JMC, Montemor MF. Comparison of the synergistic effects of inhibitor mixtures tailored for enhanced corrosion protection of bare and coated AA2024-T3. Surface and Coatings Technology 2016;303:342-51.

[111] Vaghefinazari B, Höche D, Lamaka SV, Magagnin L, Zheludkevich ML. Strong Iron complexing agents as additive in aqueous Mg-air battery. Submitted 2017.

[112] Nishioka K, Sakamoto S. Magnesium battery JP2014143191A. Japan2014.

[113] Sanchez AHM, Luthringer BJC, Feyerabend F, Willumeit R. Mg and Mg alloys: How comparable are in vitro and in vivo corrosion rates? A review. Acta Biomaterialia 2015;13:16-31.